CHEMICAL BEHAVIOUR
OF
CLINOPTILOLITE RICH NATURAL ZEOLITE
IN AQUEOUS MEDIUM

A Thesis Submitted to
the Graduate School of Engineering and Sciences of
İzmir Institute of Technology
in Partial Fulfilment of the Requirement for the Degree of

MASTER OF SCIENCE

in Chemical Engineering

by
İlker POLATOĞLU

July 2005
İZMİR

We approve the thesis of **İlker POLATOĞLU**

Date of Signature

..... **21 July 2005**
Assist.Prof.Dr. Fehime ÖZKAN
Supervisor
Department of Chemical Engineering
İzmir Institute of Technology

..... **21 July 2005**
Prof.Dr. Semra ÜLKÜ
Co-Supervisor
Department of Chemical Engineering
İzmir Institute of Technology

..... **21 July 2005**
Prof.Dr. Devrim BALKÖSE
Department of Chemical Engineering
İzmir Institute of Technology

..... **21 July 2005**
Assoc.Prof.Dr. Ahmet EROĞLU
Department of Chemistry
İzmir Institute of Technology

..... **21 July 2005**
Assoc.Prof.Dr. Metin TANOĞLU
Department of Mechanical Engineering
İzmir Institute of Technology

..... **21 July 2005**
Prof.Dr. Devrim BALKÖSE
Head of Department
İzmir Institute of Technology

.....
Assoc.Prof.Dr Semahat ÖZDEMİR
Head of the Graduate Scholl

ACKNOWLEDGEMENTS

I am grateful for the financial research support provided by Turkish Government Planning Organization (DPT), Project No: IYTE-98 K 122130 and Scientific Research Project (BAP), Project No: 2004 IYTE 06. I would like to express my sincere gratitude to my adviser, Assistant Professor Fehime Çakıcıoğlu Özkan for her guidance, support, supervision and encouragement. I am also grateful to Professor Semra Ülkü and Profesor Şebnem Harsa for their precious suggestions and recommendations.

I would like to thank all of the research scientists in the Chemical Engineering Department of İzmir Institute of Technology for their contributions to the characterization studies. I am also indented to laboratory technician Şerife Sahin for her helps in the laboratory work. I would like to thank deeply to my room mates and also especially research assistant Serdar Öztürk and Cem Göl for their friendships, supports and encouragements.

Finally, my special thanks to my family for their encouragements, patients and understandings.

ABSTRACT

In this study the chemical behavior of natural zeolite from Gördes Türkey and its Na_2CO_3 treated form was investigated in acid (hydrochloric acid, lactic acid, acetic acid) and basic (sodium hydroxide) solutions. Synthetic gastric juice (hydrochloric acid and 0.4 % pepsin at pH_i=2) was also prepared in order to examine the neutralizing capacity of zeolite for high acid concentration of stomach. The change in proton and hydroxyl concentration with time was studied by putting the different amount of zeolites into the various concentrations of acid and base solutions.

It was found that natural zeolite tended to increase the pH of acidic solution while decreased the pH of basic solution depending on the concentration of proton or hydroxyl ions in solution and zeolite amount. The proton or hydroxide ions entered to the zeolite could not balance the cations released from zeolite structure. Therefore not only ion exchange, but also adsorption, cation hydrolysis, dissolution of Al and Si, complex formation and precipitation can be occurred. The neutralizing capacity of modified zeolite with sodium carbonate was higher than untreated ones. In the study conducted with synthetic gastric juice, 0.5 g modified zeolite did not significantly affect the pepsin activity of the medium and increased the pH to 2.9 which was between the normal ranges of stomach acid (2.9-3.1). In all aqueous studies conducted by using natural zeolite there was no change observed at the surface charge of the zeolite. According to characterizations performed it is understood that there was no significant change and the structure was stable. For these reason zeolite can be used as solid buffer in aqueous medium.

ÖZET

Bu çalışmada Türkiye Gördes yataklarından çıkan doğal zeolitlerin ve bunların Na_2CO_3 ile muamele edilmiş formlarının asit (hidroklorik asit, laktik asit, asetik asit) ve baz (sodyum hidroksit) solüsyonlarındaki kimyasal davranışları incelenmiştir. Ayrıca zeolitlerin midedeki yüksek asit konsantrasyonunu nötralize etme kapasitesini araştırmak amacı ile sentetik mide asidi (pH_i=2 de hidroklorik asit ve % 0,4'lük pepsin,) hazırlanmıştır. Farklı miktarlardaki zeolitler, çeşitli konsantrasyonlardaki asit ve baz çözeltilerine atılarak zamanla sıvıdaki proton ve hidroksit konsantrasyon değişimi incelenmiştir.

Doğal zeolitin çözeltideki proton veya hidroksit konsantrasyonuna ve zeolit miktarına bağlı olarak asidik çözeltilerin pH'sını arttırma bazik çözeltilerin pH'sını azaltma eğiliminde olduğu bulunmuştur. Zeolite giren proton veya hidroksit miktarı zeolitten çıkan katyon miktarına eşit değildir. Bu nedenle sadece iyon değişimi değil adsorpsiyon, yapıdan katyon uzaklaşması, Al ve Si uzaklaşması, kompleks oluşumu ve yapı çökelmesi olabilmektedir. Sodyum karbonatla modifiye edilen zeolitlerin nötralize etme kapasitesi işlem görmemiş zeolitlere göre daha yüksektir. Sentetik mide asidi ile yapılan çalışmada 0.5 g modifiye edilmiş zeolit ortam pepsin aktivitesini önemli ölçüde etkilememiş ve solüsyonun pH'sını mide asidinin normal değerleri arasında olan (2.9-3.1) 2.9'a yükseltmiştir. Zeolitlerle yapılan tüm sıvı çalışmalarında zeolitin yüzey yükünün değişmediği gözlemlenmiştir. Yapılan karakterizasyonlara göre asit ve bazla muamele edilen zeolitlerde önemli değişiklik olmadığı, yapının kararlı olduğu ve bu nedenle sıvı ortamlarda katı tampon olarak kullanılabileceği anlaşılmıştır.

TABLE OF CONTENTS

LIST OF FIGURES viii

LIST OF TABLES x

CHAPTER 1. INTRODUCTION 1

CHAPTER 2. ZEOLITES 3

2.1. Definition 3

2.2. Structure 4

2.3. Clinoptilolite Rich Natural Zeolite 6

2.4. Application Area 8

2.5. Modification of Zeolite Structure 9

CHAPTER 3. ELECTROLYTE SOLUTIONS 11

3.1. Surface Interactions in Clinoptilolite-Aqueous Mediums 12

3.2. Literature Review in Clinoptilolite-Aqueous Medium Studies 17

CHAPTER 4. CHARACTERIZATION METHODS 22

4.1. Elemental Analysis in Solution 22

4.2. Topographic and Microstructural Examination: SEM 22

4.3. Crystallography 23

4.4. Infrared Spectrum 23

4.5. Thermal Techniques 25

4.6. Measuring Particle Surface Area by Gas Sorption; BET 25

4.7. Surface Charge Measurements; Zeta Potential 26

CHAPTER 5. EXPERIMENTAL 27

5.1. Materials 27

5.2. Methods 27

5.2.1. Modification of Natural Zeolite 27

5.2.2 Aqueous Interactions 28

5.2.3 Characterizations 31
5.2.4. Kinetics of Proton Transfer 31

CHAPTER 6. RESULTS AND DISCUSSIONS 33
6.1. Identification of Zeolitic Materials 33
6.2. Kinetics and Equilibrium Studies in Aqueous Media 38
6.2.1. Aqueous Media: Hydrochloric Acid (HCl) 38
6.2.2. Aqueous Media: Synthetic Gastric Juice (SGJ) 46
6.2.3. Aqueous Media: Acetic Acid ($C_2H_4O_2$) 49
6.2.4. Aqueous Media: Lactic Acid ($C_3H_6O_3$) 50
6.2.5. Aqueous Media: Sodium Hydroxide (NaOH) 53
6.3. Characterization of The Zeolites 56
6.3.1. XRD Studies 56
6.3.2. FTIR Studies 60
6.3.3. TGA Studies 64
6.3.4. ZP Studies 65

CHAPTER 7. CONCLUSIONS 67

REFERENCES 70

APPENDICES
APPENDIX A. REFERENCE INTENSITY RATIO (RIR) METHOD 74
APPENDIX B. PARTICLE SIZE MEASUREMENTS WITH SEDIGRAPH 76

LIST OF FIGURES

Figure **Page**

Figure 2.1. The shape of $(SiO4)^{-4}$ or $(AlO4)^{-5}$ tetrahedron (a) primary building (b) aluminosilicate structure 4

Figure 2.2. The Bronsted and Lewis acidic site of zeolite structure..... 6

Figure 2.3. a) orientation of clinoptilolite axis b) clinoptilolite framework model 7

Figure 2.4. The structural view of clinoptilolite with cation site and water Molecules 8

Figure 4.1. The structure of electrochemical double layer on a particle surface..... 26

Figure 5.1. Flow diagram of the experimental procedure..... 29

Figure 6.1. The concentration of cations in starting zeolites 34

Figure 6.2. Crystal structure of starting zeolites 35

Figure 6.3. IR spectra of Na_2CO_3 and starting zeolites 36

Figure 6.4. TGA and DTGA curves of the starting zeolites CL1, CL1*, CL2 and CL2*..... 37

Figure 6.5. The surface charge of (a) untreated (b) modified zeolites in the 0.01 M KCl solution 38

Figure 6.6. Change in pH of dilute hydrochloric acid solution after the addition of (a) as-received (b) modified zeolite (pH_i=2 T=37 ^oC..... 39

Figure 6.7. Equilibrium pH of solutions based on zeolite amount of (a) untreated (b) modified zeolites in hydrochloric acid solution system (pHi=2 T=37 ^oC)……...40

Figure 6.8. Isotherms of proton transfer for (a) untreated and (b) modified zeolites 41

Figure 6.9. Evaluation of exchange mechanism between (a) untreated (b) modified zeolite in dilute hydrochloric acid solution 43

Figure 6.10. The dissolved Si,Al and cations amount in hydrochloric acid solution when the starting zeolite in (a) as-received (b) modified form. 46

Figure 6.11. The effect of zeolite (points) and solution pH (line) on the pepsin activity in simulated gastric juice..... 47

Figure 6.12. Evaluation of synthetic gastric juice solution pH with time (Zeolite: 0.5%) 48

Figure 6.13. Change in acetic acid solution pH with time (pH_i=2, T=37 ^oC) 49
Figure 6.14. Change in lactic acid solution pH with time 51
Figure 6.15. Effect of pretreatment on lactic acid solution pH (pHi=4)..... 52
Figure 6.16. Change in pH of sodium hydroxide solution (0.00148 M) with time (pH_i=11.17 T=27 ^oC) 53
Figure 6.17. Evaluation of exchange mechanism between zeolite and sodium hydroxide solution 55
Figure 6.18. X-Ray diffraction patterns of the hydrochloric acid treated zeolites. Starting zeolite: (a) untreated zeolite, (b) modified zeolite 57
Figure 6.19. X-Ray diffraction pattern of modified and synthetic gastric juice treated zeolites 58
Figure 6.20. X-Ray diffraction pattern of untreated and synthetic gastric juice treated zeolites..... 58
Figure 6.21. X-Ray diffraction pattern of the untreated and acetic acid treated zeolite..... 59
Figure 6.22. X-ray diffraction patterns of the Lactic acid treated zeolites 59
Figure 6.23. X-Ray diffraction pattern of untreated and sodium hydroxide treated zeolites 60
Figure 6.24. FTIR spectra of the hydrochloric acid treated zeolites..... 61
Figure 6.25. FTIR spectra of synthetic gastric juice treated zeolites..... 62
Figure 6.26. FTIR spectrum of the untreated and acetic acid treated zeolite 63
Figure 6.27. FTIR spectra of the Lactic acid treated zeolites 63
Figure 6.28. FTIR spectra of untreated and sodium hydroxide treated zeolites..... 64
Figure 6.29. DTGA curve of hydrochloric acid treated zeolites 64
Figure 6.30. DTGA curve of lactic acid treated zeolites 65
Figure A.1. RIR normalization curve for quantitative determination..... 74
Figure B.1. Particle size distribution of starting zeolites (a) CL1 and (b) CL2..... 76

LIST OF TABLES

Table		Page
Table 2.1.	Zeolite types in commercial application	3
Table 2.2.	The variation of Si/Al ratio of zeolite	5
Table 2.3.	Channel characteristic and cation sites in clinoptilolite	7
Table 3.1.	Some significant studies on clinoptilolite in aqueous mediums with various characteristic	20
Table 3.2.	The parameters cause change in solution pH	21
Table 4.1.	Structure sensitivity and insensitive lattice vibrations of zeolites	24
Table 5.1.	Chemicals used in this study	27
Table 5.2.	The experimental codes used in this study	30
Table 6.1	TEC, Si/Al ratio and mean particle size of starting zeolitic minerals	33
Table 6.2.	Final pH, and proton diffusion coefficient for HCl treated samples (pH_i=2)	42
Table 6.3.	Equilibrium cation [M]e, and hydrogen [H]e amount in HCl solution ($[H]_0$=1 mmol)	42
Table 6.4.	Chemical composition of starting and HCl treated zeolites (mmol/g)	44
Table 6.5.	Dissolved Al (D_{Al} %) and Si (D_{Si} %) atoms from zeolite lattice in HCl solution	45
Table 6.6.	The effect of both amount and final solution pH on the pepsin activity in simulated gastric juice pH_i=2	46
Table 6.7.	Chemical composition of starting and SGJ treated zeolites (mmol/g)	48
Table 6.8.	Equilibrium cation [M]e, and hydrogen [H]e amount in SGJ solution ($[H]_0$=1 mmol)	49
Table 6.9.	Dissolved Al ($D_{Al\,\%}$) and Si (D_{Si} %) atoms from zeolite lattice in SGJ solution	49
Table 6.10.	Chemical composition of starting and $C_2H_4O_2$ treated zeolites (mmol/g)	50
Table 611.	Proton ($[H]_o$-$[H]_e$) and the cation exchanged ($[M]_o$-$[M]_e$) During the Lactic acid treatment. Zeolite percentage: 5%(w/v) $[M_o]_z$ = 13.90 and 18.95 meq for untreated and modified zeolite	51

Table 6.12. Dissolved Al (D_{Al} %) and Si (D_{Si} %) atoms from zeolite lattice $C_3H_6O_3$ solution 52
Table 6.13. Chemical composition of starting and $C_3H_6O_3$ treated zeolites (mmol/g) 53
Table 6.14. Equilibrium cation [M]e, hydroxide and sodium amount in NaOH solution ($[OH^+]_0$=0.296 mmol, $[H]_0=1.4*10^{-9}$ mmol, $[Na^+]_0$=0,296 mmol 55
Table 6.15. Chemical composition of starting and NaOH treated zeolites (mmol/g) 55
Table 6.16. Dissolved Al (D_{Al} %) and Si (D_{Si} %) atoms from zeolite lattice in NAOH solution 56
Table 6.17. Final pH during the hydroxide diffusion in untreated zeolite 56
Table 6.18. The surface charge of starting and acid or alkali treated zeolites 66

CHAPTER 1

INTRODUCTION

One of the most important parameter in aqueous media is pH; a measure of the amount of hydrogen ions (H^+) in a solution. Its concentration affects the solubility of many substances and the activity of most systems which requires optimum proton concentration for higher efficiency. Various chemical substances such as adsorbents and ion exchangers have been used in order to adjust pH in solutions. Proton concentration is very significant parameter for most processes such as water purification, waste treatment, food processing, cosmetics, electro coating, agricultural and pharmaceutical application. The variation of pH in a liquid system is controlled by electrostatic forces between ions (Ersoy and Çelik 2002). Other factors such as ion exchanger types added to adjust solution pH, their particle size, ion concentration, cation type, hydrodynamics of the reaction system, solvent type and heat of solution can change the pH in a liquid system and modify the behavior of ion exchangers (Mirela et al. 2002).

In contrast to other adsorbents and ion exchangers, natural zeolites (NZ) can adsorb molecules readily, slowly, or not at all depending on the size of the openings, thus functioning as molecular sieves means adsorbing molecules of certain sizes while rejecting larger ones. The ability of these molecular sieves to attract and sort molecules is also affected by the electrical charge or polarity of the molecules being sorted. NZ provides a more selective sorbent when comparing with equals which can cause the loss of necessary substances in the medium (Gomonaj et al. 2000). NZ are nontoxic material and have also the advantage of tailoring their properties (Concebcion-Rosabal and Rodriguez-Fuentes 1997). These materials are chemically stable in aqueous solutions at different pH, particularly in strongly acidic or basic media that special attention has been given to because of their technological importance. However they have small pore size, low surface area and include some impurities when compared to the synthetic ones (Mumpton 1999).

It is well established that the multiple uses of low-cost natural zeolitic materials are based on their exceptional physicochemical properties. Thus, obtaining new materials with great variety and development of their features, resulting from modifications of the bare materials, has been the topic of considerable interest during

the last years (Farias et al. 2003). If how zeolite functions affect any systems can be clarified with investigations, then the adsorption, cation-exchange, dehydration, catalytic, and biotechnical properties of zeolitic materials must therefore become a major part of a mineral scientist's portfolio (Mumpton 1999). Considering that many chemical processes are closely related to ion exchange, adsorption and catalysis, it is expected that NZ could make a significant contribution to most process especially pharmaceutical industry and medicine in the near future (Kurama et al. 2002, Castellar et al. 1998).

Proton concentration in gastric juice is determinative parameter for acidity of this media. An abnormal increase in the hydrochloric acid concentration or in the other word hyperacidity in the stomach cause decrease in pH. Such gastric disturbances are commonly treated by antacid to neutralize some extent the excess hydrochloric acid in the gastric contents (Rivera et al. 1998). Based on this fact NZ has been investigated in order to treat such gastric disturbance.

The aim of this study is to investigate the chemical behavior of clinoptilolite rich NZ in aqueous media. The kinetic study of pH was performed in order to yield some information about the mineral–water interactions and its buffering capacity. Characterization of solid and liquid phases was performed to explain the possible mechanism that could take place and how zeolite structure is affected by these interactions. The motivation of this study is the potential use of NZ as a matrix for pharmaceutical industries.

CHAPTER 2

ZEOLITES

2.1. Definition

Mineral can be defined as solid crystalline substance which is inorganic and has a specific chemical composition. Zeolite form a family of minerals, which have been known since 18th century, but they remained a strange for scientists and collectors until 60 years ago, when their unique physicochemical properties attracted the attention of many researchers.

Zeolite is crystalline, hydrated aluminosilicate of alkali and alkaline earth metals especially, sodium, potassium, calcium, magnesium, strontium and barium having an infinite, open, three dimensional structures (Mumpton 1999). It may be expressed by idealized formula as follows

$$M_{x/n}[(AlO_2)_x(SiO_2)_y].wH_2O$$

M represents the cation of valence n, x is general equal, and w is the number of water molecules. The sum of (x+y) represent the total amount of tetrahedral while the portion with [ ] defines the framework composition (Breck 1974).

Zeolites may be either obtained from mineral deposits or synthesized. Over 150 species of synthetic zeolite have been synthesized and six kind of mineral zeolites have been found in substantial quantity and purity. These are clinoptilolite (CLI), chabazite (CHA), mordenite (MOR), erionite (ERI), ferrierite (FER) and phillipsite (PHI). They generally have greater thermal stability and better resistance to acid environments than many common commercial synthetic adsorbents (Ackley et al. 2003). Commercially only twelve basic types listed on Table 2.1.

Table 2.1. Zeolite types in commercial applications
(Source: Breck 1974).

Mineral Zeolites	Mordenite	Chabazite
	Erionite	Clinoptilolite
Synthetic Zeolites	Zeolite A	Zeolite Y
	Zeolite X	Zeolite Omega
	Zeolite F	Zeolite W
	Zeolon, Mordenite	ZSM

2.2. Structure

In the zeolite structure three relative independent components are found: the aluminosilicate framework, exchangeable cations, and zeolitic water. The main building unit of the zeolite framework is the tetrahedron in which the center is occupied by a silicon or aluminum atom connected with four oxygen atoms at the corners as represented in Figure 2.1.(a) Each oxygen atom is shared between two tetrahedral. The positive charge deficiency caused by substitution of Al^{3+} by Si^{4+} is compensated by monovalent or divalent cations located together with water molecules in the channels (Figure 2.1. (b)). These exchangeable cations in the channels can be substituted easily and therefore, they are termed extraframework cations. The silicon and aluminum atoms which are not exchanged under ordinary conditions are called tetrahedra (T) or framework cations.

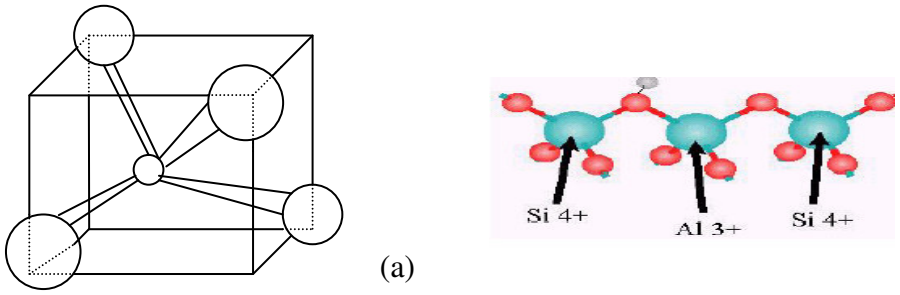

(a) (b)

Figure 2.1. The shape of $(SiO4)^{-4}$ or $(AlO4)^{-5}$ tetrahedron. (a) primary building (b) aluminosilicate structure.

Aluminosilicate framework is the most stable component and defines the structure. The content of water clearly depends on the distribution of cations. Because cations in the channels and cavities are surrounded by both water molecules and oxygen atoms. Each cation occupies its own specific site in natural forms. The hydrogen atoms are directed towards the oxygen atoms of the framework or to neighboring water molecules. All water molecules are associated with non-skeletal cations and each hydrogen is bound to a tetrahedral oxygen atom. All oxygen of the framework participates in a cation or hydrogen bond. Cations are bound more strongly by water oxygen than by framework oxygen atoms (Tsitsishvili et al. 1992, Breck 1974).

Based on the correlation Si/Al ratio zeolites are divided into high, middle, and less silica which determine their stability at different pH values (Bekkum et al. 1991).

These are low, intermediate and high silica zeolites listed on Table 2.2. The low silica zeolites represent highly heterogeneous surface with a strongly hydrophilic surface selectivity which is hydrophobic in the high silica zeolites. The acidity tends to increase in strength with increasing Si/Al ratio till a maximum values are reached at Si/Al ratio of about 6 to 7. As the Si/Al ratio increases, the cation concentration and ion-exchange capacity decrease. Low silica members are enriched with calcium, whereas high silica species are enriched with potassium, sodium and magnesium. The low silica zeolites represented by zeolites A and X are aluminum-saturated, have the highest cation concentration, and give optimum adsorption properties in terms of capacity, pore size and three-dimensional channel system. The structure of them are predominantly formed with 4, 6, 8 rings of tetrahedra. The intermediate Si/Al zeolites consist of NZ; erionite, chabazite, clinoptilolite, mordenite and the synthetic zeolites; Y, mordenite, omega and L are hydrophilic. In the intermediate silica zeolite there are 5 rings of tetrahedra. The high silica zeolites can be generated by either thermochemical framework modification of hydrophilic zeolites or by direct synthesis and there are again 5 rings of tetrahedra.

Table 2.2. The variation of Si/Al ratio of zeolite
(Source: Bekkum et al. 1991).

"Low" Si/Al Zeolites (1 to 1.5): A,X
"Intermediate" Si/Al Zeolites (2 to 5): a. Natural zeolites : erionite, chabazite, clinoptilolite, mordenite b. Synthetic Zeolites: Y, L, large pore mordenite, omega
"High" Si/Al Zeolites (10 to 100): a. By thermochemical framework modification: high siliceous variants of Y, mordenite, erionite b. By directed synthesis : ZMS-5

The acidity of zeolites is mainly caused by the presence of Bronsted acid sites. The formation of this site results from the hydrogen ions which compensate the positive charge deficiency of tetrahedral aluminum. So zeolite surface acts as a proton donor. However especially after high temperature heat treatments also Lewis acid sites may be present as shown in Figure 2.2**.** (Akpolat et al. 2004).

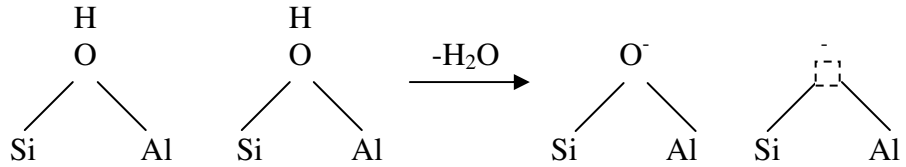

Figure 2.2. The Bronsted and Lewis acidic site of zeolite structure.

The zeolites are divided according to crystal pore size into wide-, middle- and narrow porosity. The free diameter of the channels appears to be the basic controlling factor at entering of "outside" units. The ability for their selective adsorptions behaviour of zeolite are defined by the commensurability of equivalent diameter of the zeolite crystal pores with dimension of series molecules and with this property they are related to the group of the molecular sieves (Kovatcheva-Ninova and Dimitrova 2002). Having large structural cavities and the entry channels provide them for containing water molecules, which form hydration spheres around exchangeable cations. The removal of water at 350–400°C can explain 'molecular sieve'' property of crystalline zeolites. Because during this process small molecules can pass through entry channels, but larger molecules are excluded (Mumpton 1999).

2.3. Clinoptilolite Rich Natural Zeolite

Clinoptilolite is a member of the Heulandite group NZ. Heulandite is defined as the zeolite mineral series having the distinctive framework topology and the ratio Si/Al < 4.0. Clinoptilolite defined as the series with the zeolite mineral having distinctive framework topology and Si/Al ≥ 4.0. The Si/Al ratio is the important characteristic of the heulandite–clinoptilolite minerals. It is agreed to distinguish between a low-silica calcium (Si/Al = 4.0–4.5) and high-silica sodium-potassium modifications (Si/Al =4.5–5.5) of clinoptilolite (Tarasevich et al. 2002). Its approximate chemical composition may be expressed as follows.

$$(K_2, Na_2, Ca)_3 [(Al_6Si_{30}) O_{72}].24H_2O$$

The tuff rich in clinoptilolite tuff has some impurities such as montmorillonite, celadonite, low cristabalite, chlorite, and sometimes mordenite, as well as with the high temperature minerals quartz, plagioclase, biotite and potassium feldspar (Tsitsishvili et al. 1992).

This zeolitic mineral contains three channels, limited by a system of tetrahedral rings: two channels of eight and ten tetrahedra parallel to c axis of the structure, and a third channel formed by eight member rings and connected to the other two channels as shown in Figure 2.3.

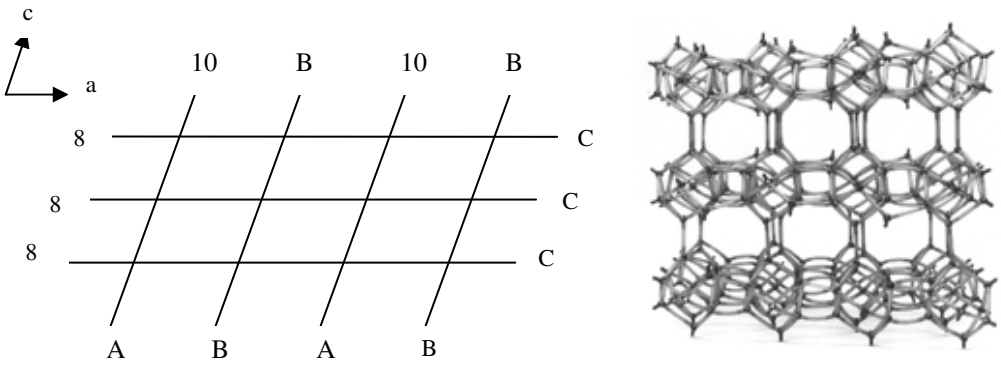

(a) (b)

Figure 2.3. a) Orientation of clinoptilolite axis b) clinoptilolite framework model (Source: Ackley and Yang 1991).

Besides the compensating cations surrounded by water molecules in the channels, the H^+ ions may also be considered as exchangeable cations present in Si–OH and Al–OH. In addition, clinoptilolite can be considered as a permanently charged mineral because of the isomorphic substitution (Ersoy and Çelik 2002). Channel characteristics and cation sites of clinoptilolite are summarized in Table 2.3.

Table 2.3. Channel characteristic and cation sites in clinoptilolite (Source: Ackley and Yang 1991).

Channel	Tetrahedral ring	Cation site	Major cations	Approx. channel
A	10/c	M (1)	Na, Ca	0.72 x 0.44
B	8/c	M (2)	Ca, Na	0.47 x 0.41
A	8/a	M (3)	K	0.55 x 0.40
B	10/c	M (4)	Mg	0.72 x 0.44

The structural view of clinoptilolite with cation site and water molecules is represented in Figure 2.4. In the clinoptilolite structure, Na^+ and Ca^{2+} ions situated in M (1) channel A and M (2) channel B. M (1) channel A is coordinated with two

framework oxygen and five water molecules while M (2), located in channel B is coordinated by three framework oxygen atoms and five water molecules in clinoptilolite lattice. K^+ is situated in M (3) site, which has the highest coordination number among all the cation sites in the unit cell. These ions have a mixed coordination sphere of water molecules and framework oxygen atoms, whereas magnesium is octahedrally coordinated only by water molecules in M (4) site. The lower exchange ability of K^+ result from strong bonding of it coordinated by six framework oxygen atoms and three water molecules. Hydration spheres are formed by the interaction between cations and water molecules and its characteristics depend on the size and charge of the cation. Hydrated radius is inversely proportional to cation radius, and divalent cations usually have a higher hydrated radius than monovalent cations (Tsitsishvili et al. 1992).

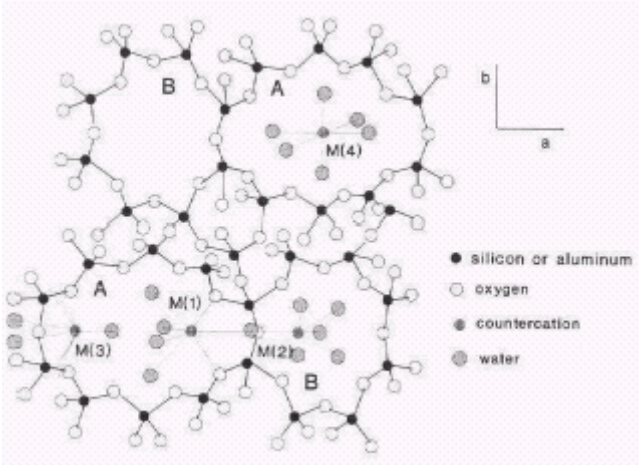

Figure 2.4. The structural view of clinoptilolite with cation site and water molecules (Source: Arcoya et al. 1996).

It is well established that the multiple uses of these materials are based on their Structure, which explain their wide range of applications in numerous agricultural and industrial areas (Rivera et al. 1998).

2.4. Application Areas

The application areas of NZ like clinoptilolite, heulandite, and mordenite are getting important due to their exceptional physicochemical properties as well as its microporous structure and low cost. Applications of NZ make use of one or more of the following properties: (*i*) cation exchange, (*ii*) adsorption and related molecular sieving,

(*iii*) catalytic, (*iv*) dehydration and rehydration, and (*v*) biological reactivity (Mumpton 1999).

From the practical point of view, acid base properties of zeolites are very convenient for catalysis applications and have been extensively used in a wide range of industrial, agricultural applications. Zeolites can also be used for waste treatment applications (Ülkü 1984) especially removal of deleterious heavy metals (Türkmen 2001). NZ can be used in the field of gas separation, drying and purification as well as pollution control, including control of water hardness (Farias et al. 2003, Rivera et al. 2000, Trgo and Pertic 2003). The use of the NZ in animal health and nutrition, and also their long-term chemical and biological stability has been studied in the literature**.** Purified NZ have demonstrated good stability in its transit through the gastrointestinal tract, and to be harmless to the human body. Based on such properties, it has been used as a raw material for different pharmaceutical forms for the treatment of several pathologies in animals and humans as well as it may simply regulate pH in the gut system, resulting in fewer or less severe stomach ailments. The other application areas of NZ are building stone as lightweight aggregate and pozzolans in cements and concretes, filler in paper, energy exchangers, and solar refrigerators (Rivera et al. 2000, Mumpton 1999).

2.5. Modification of Zeolite Structure

Tetrahedral aluminum content in the framework are responsible for the catalytic, sorptive and ion-exchange properties, and in particular the chemical and thermal stability of zeolite. It is, therefore, of particular interest to modify the Si/Al ratio of the zeolite while retaining the topology and crystallinity of the framework structure. All metal oxygen tetrahedra are accessible in principle if the pore dimensions allow. This is because they are exposed to the internal zeolite surface this makes that zeolites are ideal for all sort of modification

There are three types of modifications which can be applied to the zeolite: One of them is structural modification. In this type of modification the framework SiO_2/Al_2O_3 is changed cause a change in acidity (Bekkum et al. 1991). Zeolite is hydrated and the catives are filled with water when it is in the crystallized form. This water may be present in a physisorbed state and/or in the form of the hydration shell of

cations. These two types of water are lost over a relatively wide temperature range because of the equilibrium between the water of hydration of the cations and physisorbed water. This dehydration which can be utilized in the application of zeolites as adsorbents is endothermic and reversible. In addition to this zeolite structure is resistant to high temperature but upon dehydration several zeolites undergo structural changes and collapse of the crystal structure is observed at about 1100 ^{o}C (Weitkamp and Puppe 1999, Bekkum et al. 1991).

The second type of modification method is introduction of metal particles to the zeolite structure. Enrichment of zeolites with cations such as Na^{+}, Ca^{2+} increases the ion exchange capacities of them. This type of modification enhances its functions and increases the utility of it for various processes.

The last one is exchange of charge-compensating cations. Acid and alkali washing can be given as an example for this type of modification. Therefore it can be also necessary to improve their structure and enhance their functions (Ackley et al. 2003).

CHAPTER 3

ELECTROLYTE SOLUTIONS

So many analytical procedures are related to the solution chemistry. Some examples are partitioning process in biochemical systems, precipitation or crystallization process, desalination of water, water pollution control, food processing and production of fertilizer (Praustnitz et al. 1999). Therefore, understanding of their principle of electrolyte solution is essential.

An electrolyte is a substance which dissociates free ions when dissolved to produce an electrically conductive medium. Because they generally consist of ions in solution and electrolytes are also known as ionic solutes. Strong and weak electrolyte can be classified as their ability of dissociation. Dissociation is the separation of an electrolyte into ions of opposite charge while association is the any various process of combination, such as hydration or complex-ion formation depending on relatively weak chemical bond.

Strong electrolyte is a compound which is almost completely dissociated in solution such as HCl and NaOH. It has high conductance and slowly decreases with increasing concentration. Weak electrolyte is a compound which remains significantly partially dissociated in solution such as acetic acid ($C_2H_4O_2$), has lower conductance at any concentration, but increases with decreasing the concentration. This is due to the existence of more complete dissociation in the medium and so more ions per mole of the electrolyte in solution as the concentration of a weak electrolyte decrease (Sandler 1999, Fifield and Kealy 2000). Dissociation of hydrochloric acid and acetic acid was shown below.

$$HCl \leftrightarrow H^+ + Cl^- \qquad CH_3COOH \leftrightarrow H^+ + CH_3OO^-$$

Electrolytes generally exist as acids, bases or salts. Some chemicals can act either as an acid or a base depends on including molecule is called amphoteric behavior. In the electrolyte solution the degree of dissociation of the acid or base, complexion reaction and hence the composition of solution depends on the pH of solution. Most ionic reactions which were affected by stirring and temperature in solution occur under diffusion control. When hydrogen or hydroxyl ions in solution are being diffused to solid or generated it is necessary to control the pH of it. Therefore, ion exchange,

adsorption, complex formation and precipitation reaction can occur. These reactions are related to the solubility of solid which depends on the characteristic of solution. Solubility is the strong function of intermolecular forces between solute and solvent (Praustnitz et al. 1999). The solubility of solid in liquids depends on the energy which is necessary to break up the bonds between atoms and hence dissolution is beginning as a first step and afterwards precipitation can occur (Fifield and Kealy 2000).

Chemical bond mainly covalent bond joins two or more atoms to form a polar or nanpolar molecule. Polar molecules contain separate negative and positive charge. The degree of polarity depends upon the distance between charges with in molecule and this distance is based on bond type mainly ionic and covalent bonding. Ionic bond is the electrostatic attraction forces between the ions which have opposite sings while a chemical bond formed by sharing a pair of electrons is called a covalent bond. Covalent bond has stronger attraction than ionic bond because of electromagnetic forces which act between molecules or between widely separated regions of a macromolecule.

In polar molecules the electrons which form the covalent bond are not shared as equal and so one side is becoming more negative while the other side more positive. Briefly the link bond atoms with different electronegativity is called polar bond and the polarity increases with increasing the electronegativity difference. Polarity can also affect the reaction properties in its bond. Polar molecule of a solvent attracts polar molecules of ions of a solute to produce solution and do not attract non polar molecules which has little or no separation of charge. Non polar solvents dissolve non polar solutes but do not dissolve polar substance (Gilreath 1954).

3.1. Surface Interactions in Clinoptilolite-Aqueous Mediums

The chemical behavior of natural zeolitic material in aqueous media with different initial pH values helps to explain the mineral–water interactions. When the zeolite crystals are interact with an aqueous solution, the zeolite ions communicate with the external solution, and then solution ions begin to accumulate at the surface by attraction to the surface charge and exchange or adsorb to occupy a site in the framework structure. The cations must be smaller than the pore opening of the zeolite sutructure for exchange mechanism. Other wise they are unable to enter or leave the pore system, and ion exchange con not take place. Less hydrated and smaller ions may

be able to penetrate the pore apertures while larger ones can vary their size by temporarily losing some water molecules (Weitkamp and Puppe 1999). In addition to this the ions may react with surface functional groups forming a chemical bond or cause dissolution of Al and/or Si. They may also precipitate with just dissolved amorphous aluminosilicate surface to form a new solid phase. All of these mechanisms are both depending on solid and solution chemistry (Trgo and Petric 2003, Doula and Ioannou 2003).

One of the most important phenomena is **ion exchange** main responsible mechanism for surface interaction in zeolite-aqueous solution system. Ion exchange is a chemical reaction between two phases and necessarily stoichiometric. For instance, the exchange of divalent cations like Ca^{2+} and Mg^{2+} in clinoptilolite requires two monovalent cations for electroneutrality. Each ion removed from the solution is replaced by an equivalent amount of ion in the exchanger of the same sign by conversing electro neutrality (Tsitsishvili et al. 1992).

Ion-exchange equilibrium is attained in the system of zeolite-electrolyte solution containing a counter ion which is different from that in the ion exchanger. Then diffusion is established due to the concentration difference between A and B in zeolite and solution phases and the ion A in the zeolite is partially replaced by B:

$$\beta A_z^{\alpha+} + \alpha B_s^{\beta+} \leftrightarrow \beta A_s^{\alpha+} + \alpha B_z^{\beta+}$$

Where zeolite (z) is initially in the A form and that the counter ion in the solution (s) is B. α and β are the charges of the exchange cations B and A respectively. Reaction proceeds until equilibrium is reached. In equilibrium, both the zeolite and the solution contain both competing counter ion species, A and B**.** Most of cations within the zeolite channels are free to move and they are mobile in the external solution phase. However the "anions" within the zeolite are not free to move while the ones in the solution are free (Petrus and Warchoł 2003, Tarasevich et al. 2002, Valverde et al. 2001, Tsitsishvili et al. 1992).

Ion exchange mechanism causes both increase and decrease in solution pH based on the equation below.

$$[S\text{-}OM]_z + [H]_s \leftrightarrow [S\text{-}OH]_z + [M]_s \text{ result in increase in pH.}$$

$$[S\text{-}OH]_z + [M]_s \leftrightarrow [S\text{-}OM]_z + [H]_s \text{ result in decrease in pH.}$$

Where S → surface central metal (Si, Al) and M → cation

The overall structure of the zeolite do not undergo any changes in the ion exchange phenomena, however there are well documented cases where a phase

transformation can occur, especially in the exist of monovalent cations. The dynamics of ion exchange process can be investigated by the help of mono and divalent exchangeable cations with in the channels and cages of the zeolite structure .Clearly these two types of exchangeable cations have different motilities depending on different ion size in the possibilities of water presence (Bekkum et al. 1991).

The cations in the presence of water can also be transferred to the solution with **cation hydrolysis** mechanism. This mechanism explained below cause an increase in their concentration in solution.

$$[S\text{-}OM]_z + H_2O \leftrightarrow [S\text{-}OH]_z + [MOH]_s$$

The exchangeable monovalent; Na^+, K^+ and divalent; Ca^{2+}, Mg^{2+} cations compensate the positive charge deficiency of the clinoptilolite lattice which results from substitutions of Al^{3+} for Si^{4+}. The cation exchange capacity (CEC) of a zeolite is attributed to this negative charge and the greater the Al content, the more extraframework cations needed to balance the charge (Mumpton 1999). As an example NZ have CECs from 2 to 4 milliequivalents/g (meq/g), about twice the CEC of bentonite clay. Therefore, the ion exchange capacity of zeolite depends on the chemical composition and higher ion exchange capacity is observed in zeolites of low SiO_2/Al_2O_3 ratio. The specific ion exchange capacity varies with the structure of the zeolite and the exchange cation. One advantage of zeolites for ion exchange is the availability of a great variety of zeolites with different, but uniform, pore size, so that "ion sieving" becomes possible as mentioned before (Weitkamp and Puppe 1999). Therefore, zeolite have unusual cation selectivity superior to the other exchangers.

Main difference in the ion exchange behavior of zeolite and other exchangers (clay minerals and resin) is the microporous crystalline nature of zeolites. The behavior of cation exchange depends on some factor such as; 1) the nature of cation species, the cation size (both anhydrous and hydrated) and cation charge; 2) the temperature; 3) the structural characteristic of the particular zeolite; 4) the concentration of the cation species in solution 5) the anion species associated with the cation in the solution; 6) the solvent; 7) and the variation of pH in a liquid system (Mirela et al. 2002, Breck 1971).

Increasing of hydrogen or hydroxyl concentration in solution lead to their **adsorption** on zeolite lattice. Adsorption is a surface phenomenon which is one of the most important chemical processes in soils and soil constituents (Gilreath 1954). The composition of the zeolite framework (Si/Al ratio) and the surface area have a significant effect on the sorptive properties of the adsorbent (Kurama and

Zimmer2002). The Brønsted and Lewis theory of acidic and basic sites existing in the microporous structure is also responsible for the adsorption behavior of zeolitic minerals. This behavior is also concerned with its net charge. Therefore, not only does isomorphous Si/Al substitution account for a negative charge, but the oxygen atom in the Si–O–Al species bears a negative charge of the lattice and behaves as a proton acceptor. On the other hand the range of site energies with different sorption affinities on the surface of the zeolitic grain results in nonhomogeneous distribution of different species being adsorbed. The formation of sites with different energy is because different shape of surface crystal faces and their imperfections, such as corners, broken bonds, and edge sites, as well as amphoteric nature of hydroxyl surface groups (Trgo and Petric 2003).

Adsorption of hydrogen or hydroxyl ion to the zeolite structure causes surface protonation or deprotonation respectively. These reaction can be represented by

$$[S\text{-}OH]_z + [H^+]_s \leftrightarrow [S\text{-}OH_2^+]_z \leftrightarrow \ S + H_2O \text{ result in increase in pH.}$$

$$[S\text{-}OH]_z + [OH^-]_s \leftrightarrow [S\text{-}O^-]_z + H_2O \ \text{ result in decrease in pH.}$$

Adsorption phenomena result in some forces such as weak, physical, Van der Waals and electrostatic forces which can hold atoms, molecules or ions upon the surface of crystal or into a crystal lattice to chemical interactions. These interactions can include inner-sphere and outer-sphere complexation. When adsorption process begins, outer-sphere complexes are formed on external surface sites. The following reaction represents the outer-sphere complex.

Outer-sphere complex: rapid and revesible.

$$(\equiv S\text{–}O^-)_2 + M^{2+} \leftrightarrow (\equiv S\text{–}O^-)_2 \ \ldots \ M^{2+}$$

In basic solution of NaOH these reaction can be written as

$$\equiv S\text{–}O^- + Na^+ \leftrightarrow \equiv S\text{–}O^- \ \ldots \ Na^+$$

Inner sphere complexation leads to more stable surface groups due to the formation of covalent bonds (sharing the electrons) or some combinations of covalent and ionic bonding metal ions. The process causes a total decrease in solution pH because of realizing hydrogen cations as product. The following reactions represent inner-sphere complex for divalent M cation:

Inner-sphere complex: slow and can irreversible involve ion exhange.

$$\equiv S\text{–}OH + M^+ \leftrightarrow \equiv S\text{–}OM^+ + H^+$$

The differences between inner and outer-sphere complex are strongly depending on ionic strength. Outer-sphere complexes involve electrostatic bonding mechanisms

and, therefore, are less stable than inner-sphere surface complexes as stated by Doula and Ioannou (2002).

In the case of adsorption mechanism being dominant **dissolution or dealumination** from zeolite structure can be possible. Si/Al ratio, solution ionic strength, solution pH, temperature, physical and chemical structure of solute particles strongly affects the dissolution of silicon and aluminum (Doula and Ioannou 2003). The acidic and basic behavior of aluminosilicate structure and its interaction with hydrogen or hydroxyl ions from the aqueous solution is explained as a physicochemical phenomenon like hydrolysis of the Al–O–Si bonds and dissolution of surface layers of the zeolite particle (Trgo et al. 2003, Doula and Ioannou 2003). Ion-exchange with heat treatment and acid treatment of the 'raw' zeolite can cause such phenomena (Oumi et al. 2002).

The removal of surface functional groups from framework increased number of potential sorption sites, which precedes the process of ion exchange/adsorption into zeolite (Trgo et al. 2003). Especially Al removal known as dealumination modify the Si/Al ratio, stabilize the structure and produce the mesopores (Anna et al. 2001). Especially in acidic solution Dealumination ratio is higher and represented as

$$[\text{Al-OH}]_z + [\text{H}^+]_s \leftrightarrow [\text{Al-OH}_2^+]_z \leftrightarrow \text{Al}^{3+} + \text{H}_2\text{O}$$

The anions involved in solution may also be related to Si and Al release from the zeolite framework. Anionic ligands (A^{n-}) can be adsorbed to solids by two ways as inner-sphere complexation and outer-sphere complexation mechanisms. Outer-sphere complexation of a ligand take place when an anion (A^-) coordinate to a protonated hydroxyl or surface metal cation (Doula and Ioannou 2003).

$$\equiv\text{S–OH}^+_2 + \text{A}^{n-} \leftrightarrow \equiv\text{S–OH}^+_2 \ \ldots \ \text{A}^{n-}$$

Inner-sphere complexation occurs in two steps. Initially protonation of surface Lewis acid sites then protonation, hydroxyl ligand exchange can occur (Doula and Ioannou 2003).

$$\equiv\text{S–OH} + \text{H}^+_{aq} \leftrightarrow \equiv\text{S–OH}^+_2 \qquad \equiv\text{S–OH}^+_2 + \text{A}^{n-} \leftrightarrow \equiv\text{S–A}^{(-n+1)}$$

Inner-sphere complex with a ligand such as Cl^- facilitates the detachment of a central metal ion and enhances the dissolution based on excess electron density shift which increases the surface protonation. Similarly, surface protonation facilitates the detachment of a cationic surface group into the solution, because it leads to highly polarized interatomic bonds in the immediate proximity of the surface central ions (Doula and Ioannou 2002).

Cations or anions in solution form surface coverage by being adsorbed to the surface of a mineral. At low sorbate cation concentrations surface complexion is dominant mechanism. In the case of high sorbate cation concentration the amount of a metal cation or anion sorbed on a surface increases result in nucleation and the formation of distinct entities or aggregates on the surface. As surface coverage increases **surface precipitation** becomes the dominant mechanism (Doula and Ioannou 2002, Stumm 1992). The formation of large aggregates is necessary in order to precipitate a colloid. This formation is prevented by the mutual repulsion of the ions which carry a similar electric charge. Therefore, it is obvious that to coagulate a colloid it is necessary to neutralize the charges carried by the dispersed particles.

The precipitation or coagulation of a solution is affected by the ions with opposite charge. The ions with multiple charges are more effective than ions with single charges in the coagulation phenomena. Trivalent ions are more effective than divalent ions, and divalent ions are more effective than univalent ions. But that is not means that a divalent ion has twice coagulation power than that of a monovalent ion.

On the other hand every electrolyte required minimum concentration to cause the precipitation of aggregates. When the amount of electrolyte added a solution greatly exceeds the quantity required for coagulation, the exceed may actually stabilize the solution by reversing its charge (Gilreath 1954).

3.2. Literature Review on Clinoptilolite-Aqueous Medium Studies

Natural zeolitic material has been studied for most investigations in the literature due to their distinctive properties as summarized in Table 3.1. In the electrokinetic properties of clinoptilolite study performed by Ersoy and Çelik (2002), zeta potential measurement have been conducted in electrolyte solution with different pH indicating that clinoptilolite particle has negative surface charge even in acidic condition. Changing of solution pH was also observed depending on initial proton concentration.

Recently in gastric juice and ulcer treatment, NZ have an important role due to their acidic basic chemical behavior and resistance in body fluid. Such gastric disturbance are commonly treated by antacids like NZ reported by Rivera et al**.** (1998). Also zeolitic products and drugs can be simultaneously administrated to a patient without any loss of the individual pharmaceutical effects of each substance during their

transit through the gastrointestinal tract reported by Farias et al. (2003). This is an important result from the pharmaceutical point of view in order to decrease the hydrochloric acid concentration in the gastric content.

In the direct acid treatment study performed by Anna et al. (2001), change in zeolite structure was observed. Increasing of Si/Al ratio was due to the dealumination procedure which is the removal of Al from zeolite lattice.

Özkan and Ülkü (2004) investigated the effect of HCl treatment on water vapor adsorption characteristic of clinoptilolite rich NZ. It is found that the Langmuir surface area and ultra-micropore volume depend on the degree of the removal of the aluminum from structure which was very sensitive to HCl solution concentration at high treatment temperature.

Trgo and Petric (2003) examined the removal of zinc ions from water. The removal of zinc in the acidic condition was due to the ion exchange and partly adsorption of H ions to the zeolite result in increase in pH. In basic condition the removal of zinc ions was due to complexion of zinc with hydroxyl ions result in precipitation and also the attack of OH ions to the zeolite structure. These behaviors cause a decrease in pH.

In the study of silver supported on Mexican zeolite as an antibacterial material performed by Rivera–Garza et al. (2000), the antimicrobial effect of this zeolite exchanged with silver ions was investigated. It was found that this zeolitic mineral eliminated the pathogenic microorganisms E. coli and S. faecalis from water with the highest amount of silver supported on the mineral.

Ponizovsky and Tsadilas (2003) investigated the lead retention by alfosil and clinoptilolite in various pH values. They found that clinoptilolite sorbed 20-30 times more Pb than soils. Based on balance between sorbed and displaced ions, ions exchange was considered as possible mechanism for the removal of Pb.

Doula and Ioannou (2001) studied the copper adsorption and Si, Al and the other exchangeable cations from zeolite structure. In this study copper adsorption was found to increase with increasing the solution pH and with decreasing the electrolyte concentration. The characterization of zeolite with FTIR and X-Ray diffraction techniques was used in order to better understanding of possible mechanism in this study. In the study conducted by same author in 2002 the effects of electrolyte anion on Cu adsorption- desorption by clinoptilolite was investigated. Three different electrolytes KCl, KNO_3, and K_2SO_4 were used. It is observed that the surface was able to hold the

$Cl^-$and NO_3^- ions via a surface complexation mechanism and this process enhanced the adsorption of Cu^{2+} due to the increase in surface negative charge.

In the other study reported by Castellar et al. (1998), zeolite was selected to improve the production of ethanol fermentation in the presence of zeolite. During this production the medium of pH decrease. Maintaining pH around 3.7 leads to consumption of all of the glucose in the fermentation so higher ethanol concentration can be obtained in the presence of zeolite. Thus, zeolite can act as a pH regulator, due to its ion exchange.

Table 3.1. Some significant studies on clinoptilolite in aqueous media with various characteristic

References	Aqueous medium	Aim	Outcome
Bahri and Çelik 2002	Electrolyte solutions	Investigation of zeolite surface charge	Neutralizing the medium
Rivera and Rodriguez 1998	Acidic and basic solutions	Treatment of gastric disturbance	At lower pH increasing, at higher pH decreasing.
Farias et al. 2003	Drug solution	Simultaneously administration without any loss in individual effect	No interactions between zeolite and drugs
Özkan and Ülkü 2004	Acidic solutions	Investigate the effect of HCl treatment on water vapor adsorption characteristic of clinoptilolite	Change in surface area and micropore volume depends on dealumination
Anna et al. 2001	Acidic solution	Determining the acid resistivity of zeolite	Dealumination of structure by acid concentration
Rivera –Garza et al. 2000	Photogenic microorganisms-containing solution	Investigate the antimicrobial effect of silver supported Mexican zeolite	Removal of photogenic microorganism from water
Trgo and petric 2003	Zn-containing solutions	Treatment of water	Removal of Zn depends on pH
Ponizovsky and Tsadilas 2003	Lead containing solution	Lead retention by alfosil and clinoptilolite	Clinoptilolite has higher sorption capacity
Doula and Ioannou 2001	Copper-containing electrolyte solution	Investigate the effect of solution pH and electrolyte solution on copper adsorption mechanism.	Increasing of copper adsorption with increasing the solution pH and with decreasing the electrolyte concentration.
Doula and Ioannou 2002	Copper-containing various electrolyte solution	Investigate the effect of electrolyte anions on copper adsorption mechanism.	Enhancement of copper adsorption by the surface complexation mechanism of anions
Castellar et al. 1998	Glucose-containing solution	Improve the production of ethanol fermentation	pH regulation

The chemical structure of zeolite, its crystal content and particle size, the concentration of it in solution and solution chemistry affect change in pH and consequently their results for all of these studies. These parameters are summarized in Table 3.2.

Table 3.2. The parameters cause change in solution pH.

References	Bahri and Çelik 2002	Charistos et al. 1997	Rivera and Rodriguez 1998	Trgo and petric 2003	Doula and Ioannou 2001
Aqueous medium	HCl and NaOH solutions	KCl, HCl and KOH solutions	Synthetic gastric juice 90-92	Zn-containing solutions	Cu-containing various electrolyte solution
Solid/liquid Ratio	1/20	1/100	1 g zeolite * 0.4 g Na_2CO_3 rich zeolite	1/100	1/200
Clinoptilolite Content (%)	90-92	-	70	50<	-
Particle size (μm)	-	20-90	37-90	100-500	-
Si/Al ratio	-	1.85	5.8	4.8	5.03
Initial Ph	2- 6-11.5	2.14-5.30-11.3	1.57-* 1.57	1.99-3.97-11.1	2.97-5.78-9.36
Final pH	8.7-9.2-10	4.15-7.62-10.53	2.3-3	6.63-8.19-8.41	4.16-7.01-3.25

CHAPTER 4

CHARACTERIZATION METHODS

The characterization of a zeolite provides information about its chemical composition, its structure and morphology, the ability of sorbing and retaining the molecules (Jentys and Lercher 2001). Characterization is indispensable in order to understand the phenomena occurred in any system. The control of product quality and its development can be possible by the help of characterization (Fifield and Kealey 2000). The fundamental task to be performed by characterization is the translation of chemical information into a observable form (Ewing 1985).

4.1. Elemental Analysis in Solution

This technique can be applied to determine the elements in solution and so give some information about elemental composition of a substance. It can detect lost of elements at ones and also determine minor or trace elements in the solution (Fifield and Kealey 2000). The fusion method is applicable for the decomposition of geological samples in order to analyze it by inductively coupled plasma atomic emission spectroscopy (ICP-AES). Lithium tetraborate or lithium metaborate is used to decompose the samples. The fused sample is dissolved in specific concentration of nitric acid and the resultant solution analyzed directly (Liberatore 1993).

4.2. Topographic and Microstructural Examination; SEM

There are numerous techniques for determining the elemental composition of a sample. However scanning electron microscopy (SEM) is an important tool for examination and analysis of microstructural and microchemical characteristics. This technique requires quantitative analysis and non-destructive techniques to detect most elements (Lawes 1987). The advantages of SEM include high-resolution imaging, greater magnification which provides textural information and much greater depth of field. Imaging can be obtained by using secondary electrons for the best resolution of fine surface topographical features. Alternatively, imaging the surface with

backscattered electrons provides contrast based on atomic number to resolve microscopic composition variations, as well as, topographical information. Qualitative and quantitative chemical analysis information is also obtained using an energy dispersive x-ray spectrometer

4.3. Crystallography

X-Ray diffraction enables some information about crystal structure, crystallite size, location and concentration of exchanged cations and crystallinity of a zeolite sample. The diffraction of X-ray provides identification of crystal materials while the adsorption of X-ray gives some information about the adsorbing material. Giving some information about the quantitative determination of relative amounts in solid is also possible (Ewing 1985). However obtaining the information on non-periodic properties of the crystals such as lattice defects, stacking faults and hydroxyl groups resulting from an incomplete condensation of Si-O-Si linkages during the synthesis is not possible (Jentys and Lercher 2001).

4.4. Infrared Spectrum

IR spectra which can estimate the order and disorder problem in zeolites is a useful technique in obtaining crucial information about the structure of zeolites. The position of the ring band depends on several factors. These are the number of ring member, Al/Si ratio, kind of nontetrahedral cations, degree of ring deformation, degree of zeolite hydration and arrangement of structure (Mozgava et al. 1999).

The bond frequencies in the range 200-1200 have been classified in two ways. One of them is structure sensitive oscillations of external tetrahedral bonds, the other one is structure insensitive oscillation of individual tetrahedra. On the basis of this classification the bonds ascribed to 3 modes: antisymmetric stretches (1200-950 cm^{-1}). Symmetric stretches (720-650 cm^{-1}), and deformation stretches (490-500 cm^{-1}). The structure sensitive and insensitive lattice vibration of zeolites is represented by Table 4.1.

The bonds observed at 1040-1100 cm^{-1} are more intense ones caused by O-Si (Al)-O-bond vibrations. The degree of zeolite can be estimated on the basis of the band

shape changes in the region of 1055 cm^{-1}. This O-T-O band is sensitive to the content of the framework silicon and aluminum so it is very also sensitive to the dealumination degree. Dissolution of Al and Si causing a shift of v_{O-T-O} toward higher frequency while increasing of the number of the ring members result in shifting of the characteristic rind band to the lower wave number .

Table 4.1. Structure sensitivity and insensitive lattice vibrations of zeolites (Source: Jentys and Lercher 2001).

Structure insensitive vibrations	**Wavenumber [cm^{-1}]**
Asymmetric stretching vibrations	1200-1000
Symmetric stretching vibrations	850-700
Bending vibrations	600-400
Structure sensitive vibrations	
Asymmetric stretching vibrations	1050-1150
Symmetric stretching vibrations	750-820
Double ring vibrations	500-650
Pore opening vibrations	300-420

The other relative bonds at 440 do not undergo much change as the bond in 1055 cm^{-1}. The intensity of the band at about 410-470 cm^{-1} does not depend on the degree of crystallization. So the ratio of the intensity of this bands describes the degree of amorphization. Cations do not much alter the character of the spectrum of the clinoptilolite in the range of 400-800 cm^{-1} and 900-1200 cm^{-1}

The adsorption bond at 550-650 cm^{-1} relate to oscillations of chains of aluminoslicate oxygen tetrahedral while the band at 750-820 cm^{-1} is clearly results from symmetric vibration of the Si-O band. Characteristic for the Si-O-Si and Si-O-Al bridges can be expected in the region of 690-800 cm^{-1} (Özkan and Ülkü 2004, Doula and Ioannou 2003, Tsitsishvili et al. 1992).

In the region of deformation vibrations, one 1620 cm^{-1} band is observed for all zeolites. The band in 1690 cm^{-1} result from small amount of water is a deformation mode of hydroxonium. The intensity of high frequency bands at 3100-3700 cm^{-1} can be also observed depending upon the radius, mass and charge of the cations (Tsitsishvili et al. 1992). The Band in between 3680 and 3550 cm^{-1} are attributed to the bridging OH

groups in Si–OH–Al and are results from the location of hydrogen atoms on different oxygen atoms in the framework (Doula and Ioannou 2003).

4.5. Thermal Techniques

Thermal methods provide qualitative or quantitative analytical information by the effect of heat on a sample. Thermal analysis may be explained as a group of techniques. In these techniques the temperature in the specific atmosphere is programmed while the property of this sample is monitored against time or temperature (Fifield and Kealey 2000). Thermogravimery (TGA), derivative thermogravimery (DTG), differential thermal analysis (DTA) and scanning calorimetry (DSC) are some of this method. TGA is a technique that the sample weight can be followed in a specific period of time while its temperature is being raised gradually (Ewing 1985).

Many materials give specific curves when they are heated over the range of temperatures. This change can be due to the particular thermal event such as loss of water of crystallization. If the thermograms are complex and the changes are obscure then DTG can be valuable for interpretation (Fifield and Kealey 2000).

4.6. Measuring Particle Surface Area by Gas Sorption; BET

When metal cations exchange with proton the pores of zeolite undergo dimensional changes (Kurama et al. 2002). Acid treatment of zeolite changes the porosity, total surface area of the adsorbent, the micropore surface area, and so adsorption capacity of it (Gomonaj et al. 2000; Tsitsishvili et al. 1992). Adsorption measurement with molecules of different size gives direct information about the dimension of the pore system. By enveloping each particle with an adsorbed gas it is possible to determine the surface area of a sample. Therefore the BET surface area is reported for zeolites (and other microporous materials) and can be used as a purely empirical value to compare the quality and porosity of material (Jentys and Lercher 2001).

4.6. Surface Charge Measurements; Zeta Potential

Adsorption of ions, the formation of structural OH^- groups (upon dealumination) or H_3O^+ ions (proton-zeolite water interaction) can cause changes in the surface charge of soil particles (Ponizovsky and Tsadilas 2003, Tsitsishvili et al. 1992). These phenomena upon the surface of a particle result in an electrical unbalance in the solution as shown in Figure 4.1.

The formation of secondary layer of ions with opposite charges which surrounds the colloidal particle in solution corrects this unbalance. The resulting electrical double layer resembles a parallel- plate condenser and accounts for the stability and electrical properties of electrovalent solutions. The primary layer of the charges on the particle is monomolecular and immovable, whereas the secondary layer is diffuse and mobile. The potential difference between the mobile liquid layer of ions immediately surrounding the particle and the immovable liquid layer of ions attached to the surface of the particle is called zeta potential. It is shortly the differences between primary adsorption layer and secondary adsorption layer (Ersoy and Çelik 2002, Gilreath 1954).

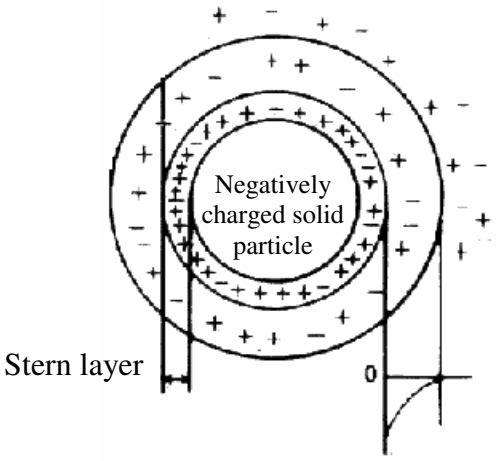

Figure 4.1. The structure of electrochemical double layer on a particle surface.

CHAPTER 5

EXPERIMENTAL

5.1. Materials

In this study two sedimentary zeolitic tuff from Gördes (Manisa) deposit supplied by Enli Madencilik Company was used. The zeolites (CL1 and CL2) were ground and dry sieved to obtain the fraction between 38-106 μm. The chemicals used in the experiments were tabulated in Table 5.1.

Table 5.1. Chemicals used in this study.

Chemicals	Specifications
Sodium carbonate (Na_2CO_3)	Merck, 99.9 % purity
Hydrochloric acid (HCl)	Merck, 37 % purity
Acetic acid ($C_2H_4O_2$)	Panreak, 99.5 % purity
Lactic acid ($C_3H_6O_3$)	Panreak, 90 purity
Sodium hydroxide (NaOH)	Sigma, 98.4 purity
Pepsin	Merck, ≥ 0.7 FIP U/mg at pH: 1.6

5.2. Methods

5.2.1. Modification of Natural Zeolite

Chemical treatment was applied to the clinoptilolite rich NZ by using 0.5 M Na_2CO_3 solution with a solid liquid ratio of 1:2 for 1 h. This treatment was conducted at 100 ^oC at atmospheric pressure under reflux condition. Then one of the chemically treated clinoptilolite was submitted to washing step consisted of a 5 min agitation in deionize water. After centrifugation with Sigma 6K15 model centrifuger at 9000 rpm for 20 minutes and drying at 120 ^oC for a night, the modified clinoptilolite (CL1*) was obtained. The obtaining materials were used for dilute HCl treatment. The other experiments were performed by using zeolitic mineral taken from similar source (CL2)

and its modified form. Same procedure was applied to CL2 but after chemical treatment, the washing step was not applied and CL2* was obtained. The particle size distribution of zeolitic minerals was determined by using Micromeritics 5100 model sedigraph.

5.2.2. Aqueous Interactions

The untreated and pretreated natural clinoptilolites CL1, CL2, CL1*, CL2* were interacted with different electrolyte solutions at various solid/liquid ratios in order to analyze the change in proton concentration of solution with time and to understand their neutralizing capacities. The reason using different amount of zeolitic tuff is to see the effect of zeolite concentration on proton uptake mechanism. The experimental codes were prepared in Table 5.2. depending on the type of electrolyte solution, the characteristic of natural clinoptilolite, solid/liquid ratio, pH, and temperature. These experiments were carried out in a shaker (GLF 1092) with a shaking rate of 200 rpm by using 744 Metrohm pH meter. The change in pH of the solutions recorded in every 10 min at the beginning and the time interval was increased gradually after words. Solid and liquid parts were separated by using Sigma 6K15 model centrifuger when the solution pH reached to equilibrium. Then solid parts (clinoptilolite) (Table 5.2.) were dried in room temperature and kept in plastic beaker while liquid parts were kept in glass beaker for characterizations. The experimental procedure was summarized as a flow diagram in Figure 5.1.

Gastric disturbance caused by hyperacidity is high HCl concentration of gastric juice. In order to normalize such excess HCl concentration natural clinoptilolite was used. Synthetic gastric juice was prepared by using HCl and pepsin with 0.4 % concentration. Then different amount of both natural and chemical treated clinoptilolite was used in order to increase medium pH. The experiment was conducted at 37 ^{o}C for 2 h and for the solution proton concentration was reached equilibrium. By this way the neutralizing capacity of both natural and chemical treated clinoptilolite was determined to be dependent on final solution pH. It is important to note that not only solution proton concentration but also the properties of simulated gastric juice were effective parameter on pepsin activity in that solution. So it is necessary to determine the pepsin amount of simulated gastric juice in respect to maintenance of this media. Pepsin activity was

evaluated by using UV absorbance spectrum between 200-400 nm as a function of zeolite amount and pH. The absorbance of the pepsin solution at 250 nm was taken as the pepsin activity.

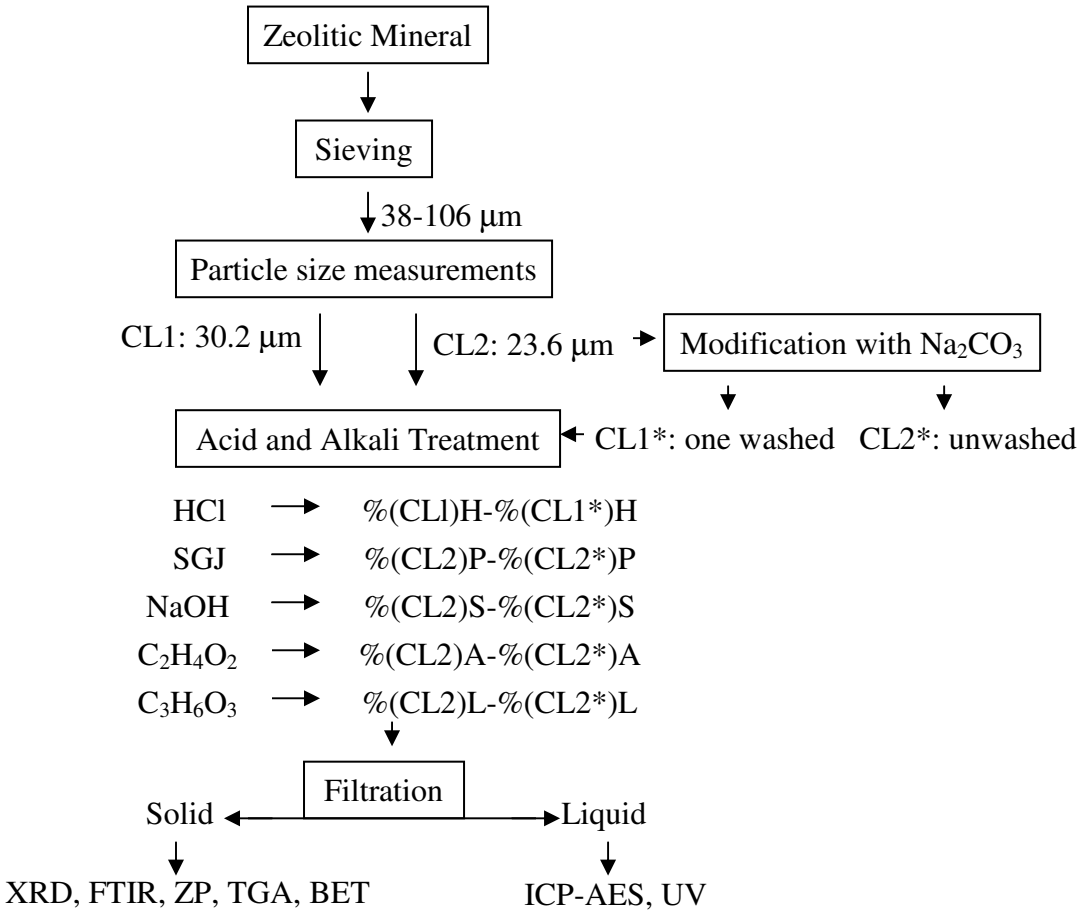

Figure 5.1. Flow diagram of the experimental procedure

Table 5.2. The experimental codes used in this study. #: two hours treatment.

Aqueous Medium	**Starting Zeolite**	**Temperature (^oC)**	**Zeolite percentage in liquid (%)**					
			0.2	**0.5**	**1**	**2**	**5**	**10**
HCl	CL1	37	0.2 (CL1)H		1 (CL1)H	2 (CL1)H	5 (CL1)H	10 (CL1)H
HCl	CL1*	37	0.2 (CL1*)H		1 (CL1*)H	1 (CL1*)H	5 (CL1*)H	10 (CL1*)H
$C_2H_4O_2$	CL2	37						
HCl + Pepsin (%0.4)	CL2	37					5 (CL2)P#	
HCl + Pepsin (%0.4)	CL2*	37		0.5 (CL2*)P	1 (CL2*)P#			
NaOH	CL2	27			1 (CL2)S		5 (CL2)S	10 (CL2)S

Aqueous Medium	**Starting Zeolite**	**Temperature (^oC)**	**pH_i**	**5 % zeolite percentage in liquid**
$C_3H_6O_3$	CL2	37	4	5 (CL2)L4
$C_3H_6O_3$	CL2*	37	2	5 (CL2*)L2
$C_3H_6O_3$	CL2*	37	4	5 (CL2*)L4
$C_3H_6O_3$	CL2*	37	5.5	5 (CL2*)L5.5

5.2.3. Characterizations

The starting, acid and alkali treated zeolites were characterized with various techniques, including ICP-AES, UV, XRD, FTIR, TGA, BET, and Zeta sizer. Shimadzu 1601 model UV Spectrophotometer was also used between 200-400 nm in order to see the concentration of pepsin in synthetic gastric juice. Original and modified zeolite had to be digested before analyzing their chemical composition in an ICP-AES (Varian ICP 96). In this respect, 0.1 g of sample was mixed with 1 g lithium tetraborate, fused in furnace at 1000 ^{o}C for 1 hour and then cooled. Final liquid phase was completed to 250 ml with necessary amount of 1.6 M HNO_3 and deionize water. The standard solutions and blank was also prepared with the same proportion of HNO_3 solution.

Mineralogy of the original zeolitic tuff and the crystallinities of the acid treated clinoptilolite were determined by powder X-ray Diffraction techniques (Philips X-Pert Pro) using CuKα radiation in the range of 2θ: 2^{o}-40^{o} with 0.2^{o} step size. The infrared spectra of the sample were recorded at room temperature by using KBr (1/200) pellet technique in Digilab FTIR- FTS3000MX device. The background correction was applied to normalize the spectrum. Thermal analysis was applied by heating the sample until 1000 ^{o}C with the flow rate of 40 ml/min under nitrogen gas atmosphere by using a TGA (Shimadzu 51/51H). The BET surface area of zeolites was measured by using volumetric adsorption device (Micromeritich ASAP 2010) with nitrogen at 77 K. Samples were degassed at 300 ^{o}C up to 10^{-5} hg vacuum before the analysis of zeolites. 3000 HAS model zeta sizer was also used in order to determine the surface charge of the zeolite particle in the solution of 0.01 M KCl. The solution pH was adjusted by using NaOH and HCl.

5.2.4. Kinetics of Proton Transfer

For a time of contact, t, proton in the solution was replaced by cations in the zeolite with a speed which was controlled by diffusion in the zeolite structure. The time t_e is that required to achieve equilibrium between the zeolite and the solution. In the time interval t_0 to t_e, proton from solution are exchanged with cations from the surface of the zeolite particle by an intradiffusional mechanism. It was ascertained that diffusion

coefficient are determined not only by geometric sizes, but also by the nature of molecules, the intensity of their interaction with adsorption centers in the zeolite.

The change in proton concentration of the solution was used to understanding the kinetics of the exchange process. The rate curves obtained for each zeolite percent was analyzed by using the equation given below to compute the diffusion coefficient (D_o) which is independent of concentration in the absence of the surface barrier as proposed by Barrer (1980). For ion exchange process

$$I_0 = \int \left(1 - \frac{H_t}{H_\infty}\right) dt = \frac{r_0^{\,2}}{15 D_0} \qquad (5.1.)$$

Where r_o is sphere particle radius, I_0 is the area above the rate curve, H_t and H_∞ are, respectively, the amount of proton transferred to zeolite at any time and t infinite.

CHAPTER 6

RESULTS AND DISCUSSIONS

6.1. Identification of Zeolitic Materials

In this study, zeolites were used in as received (CL1 and CL2) and modified forms (CL1* and CL2*). These zeolites were characterized with different techniques to acquire the information about chemical composition of zeolitic material, surface properties, as well as its crystal structure.

The total exchange capacity (TEC) of the zeolites, according to their chemical composition is calculated and presented in Table 6.1. The TEC values represents the amount of exchangeable cations, which are considered to be Na^+, K^+, Ca^{2+}, and Mg^{2+}.

Table 6.1. TEC, Si/Al ratio and mean particle size of starting zeolitic minerals.

Code	Si/Al ratio	TEC (meq/g)	Mean particle size (μm)
CL1	4.03	2.49	30.30
CL1*	4.04	3.06	nd
CL2	3.83	2.77	23.62
CL2*	3.82	3.79	nd

nd: not determined.

CL1 has less exchangeable cations to compensate the positive charge deficiency results from the low Al atom. So the CL1 has higher Si/Al ratio and lower exchange capacity when compared with the sample CL2 (Table 6.1.). The Si/Al ratio is significant for the classification of the zeolitic material as Heulandite-Clinoptilolite rich. The material can be classified as high-silica heulandite, low-silica clinoptilolite and high-silica clinoptilolite for the Si/Al range of 3.5-4, 4.0-4.5 and 4.5-5.5 respectively (Tsitsishvili et al. 1992). Modification of NZ is not effective on Si/Al ratio but on TEC. This is because of the high stability of the structure against to heat treatment. TEC was very high for modified zeolite (CL2*) determined by ICP-AES. This is because after the treatment with Na_2CO_3 no washing step was applied for that zeolite. TEC of zeolitic material (CL1 and CL2) increased 22.89 % and 36.82 % respectively with modification due to the rich Na^+ content of zeolitic material. Similar observation was found in the

study which NaCl was used to prepare near homoionic Na-form of clinoptilolite performed by Top (2001). Application of washing step caused to low increase in TEC of first deposit (CL1).

The concentration of cations in starting zeolites determined was also presented in Figure 6.1. The amount of Na^+ ions increased while the other cations decreased after the modification of zeolitic material with Na_2CO_3. However there was no balance between the increased amount of Na^+ and the decreased amount of other exchangeable cations. This is not only ion exchange but also outer-sphere complexion of Na^+ with surface functional groups. The excess amount of Na^+ cations can exchange with the

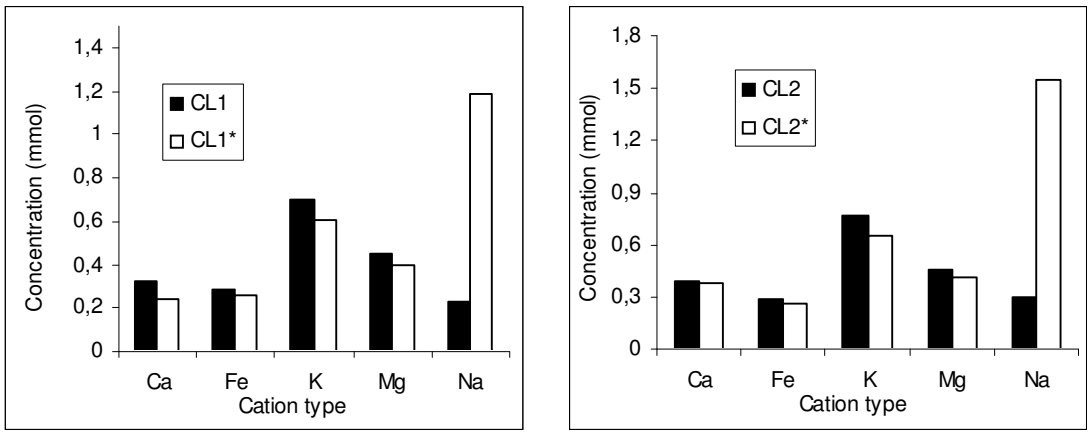

Figure 6.1. The concentration of cations in starting zeolites.

The monovalent and bivalent cation content ratio ([Na+K]/[Ca+Mg]) of the zeolitic material was calculated as 1.03 and 1.25 for CL1 and CL2 respectively. Therefore, the starting zeolite is named as low-silica clinoptilolite depending both on Si/Al ratio and cation content.

Clinoptilolite content was determined by using Relative Intensity Ratio (RIR) methods. The content of clinoptilolite was found as 55.5 % and 58.5 % for the zeolites of CL1 and CL2 respectively.

The specific surface area (BET) of as-received zeolites is 31.90 m^2/g and 54.34 m^2/g for CL1 and CL2 respectively.

Figure 6.2. shows the X-Ray diffraction of CL1 and CL2 before and after modification. Besides the characteristic peak of clinoptilolite at 9.8^o and 22.3^o (marked as CL in Figure 6.2) some new peak on the pattern of CL2* was observed. In Rivera's similar study (1998), the new peaks were formed corresponding to the complex rich in carbonate ($Na_2CO_310H_2O$ or $Na_2Ca(CO_3)_25H_2O$). The new peaks observed in our study

corresponding to the albite high ($Na[AlSi_3O_8]$) (at 27.57°, 28.56°, 28.83°, 2θ) and sodium aluminum oxide ($Na_7Al_3O_8$) (the peak at 36.03° 2θ). According to XRD results only Na^+ (not CO_3^-) ions leads to formation of the crystal structure with extraframework Al and Si atoms in the zeolite lattice.

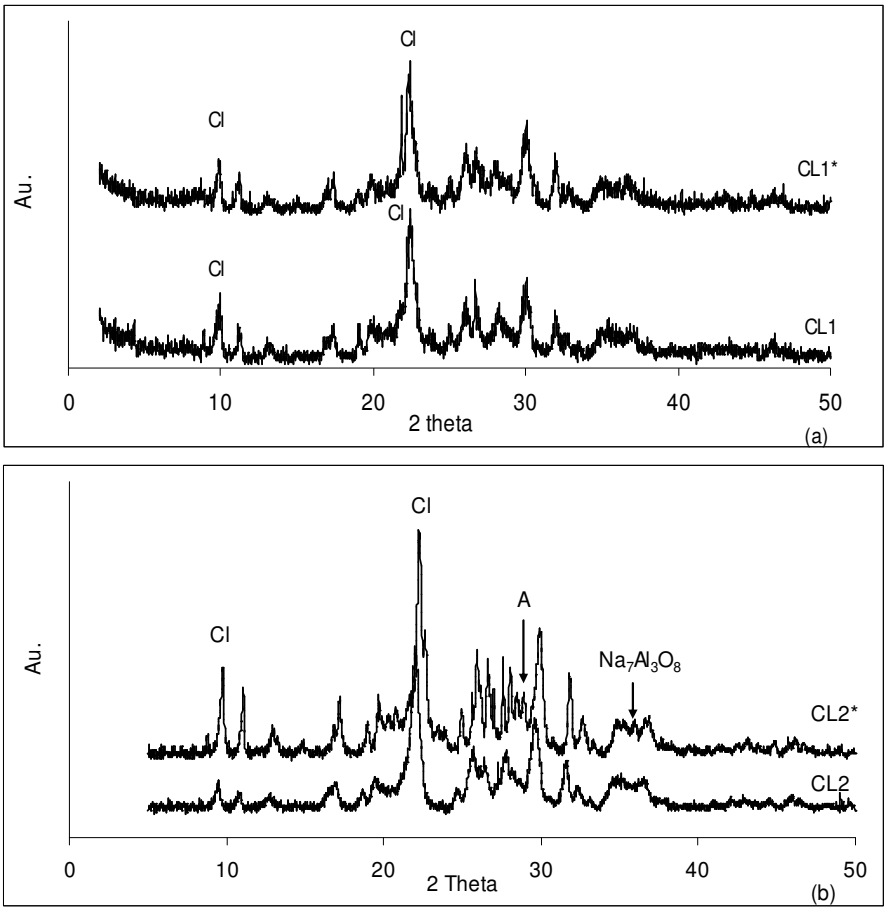

Figure 6.2. Crystal structure of starting zeolites.

The other methods FTIR and TGA were used in order to understand the changes in natural clinoptilolite structure resulting from modification. In FTIR analysis the main band observed at 1498 cm^{-1} for Na_2CO_3 detected as small vibration on modified zeolites (CL1* and CL2*) as shown in Figure 6.3. The intensity of this band was higher for the zeolite CL2* which is not washed after pretreatment (Figure 6.3. (b)).

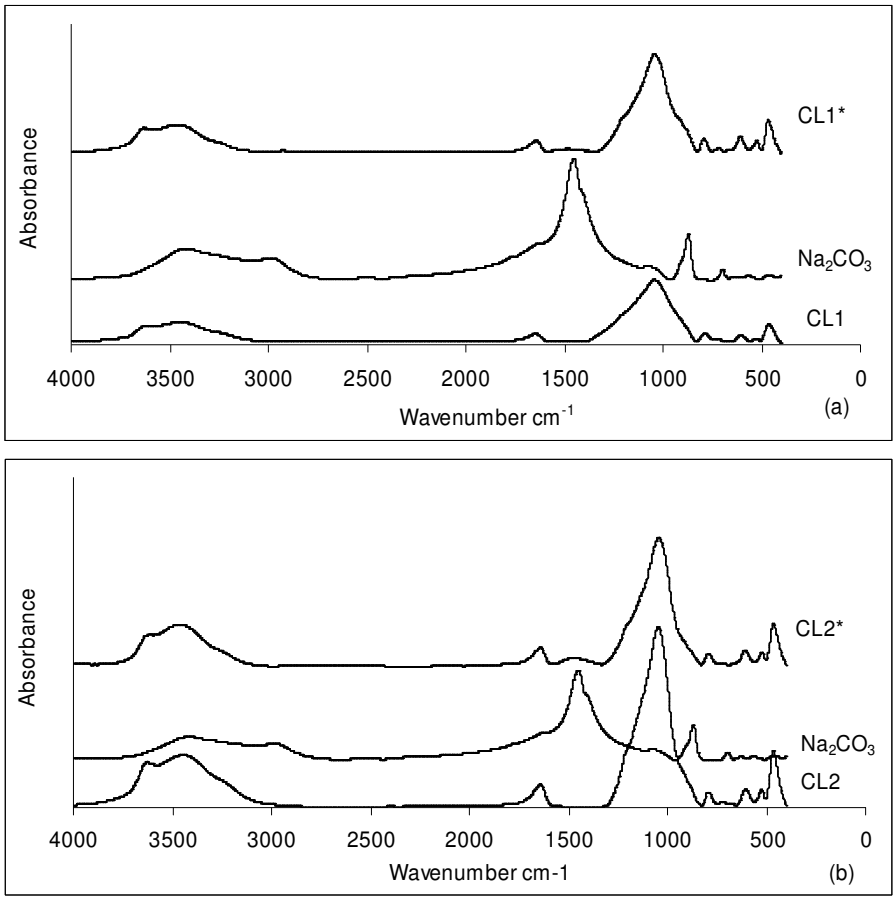

Figure 6.3. IR spectra of Na_2CO_3 and starting zeolites.

To detect carbonate in zeolite structure the thermal gravimetric analysis was also applied. The first peak is related to removal of water in the zeolite. The second peak observed between 600-710 ^oC related to decomposition of carbonate (Figure 6.4.).

The TGA termograms of the starting zeolites showed water loss which varied with the treatment. The DTGA thermograms showed a water loss in the 60-120 ^oC range due to the weakly bond water, with varying the temperature of the peak. The DTGA thermograms showed another weight loss in the 120-200 ^oC range due to the water located in the zeolite cavities and bound to the nonframework cation.

The maximum amount of water desorption, determined by TGA occurred 50 ^oC and no phase transformation was observed below 600 ^oC. The weight loss indicating water content of zeolite are 11 %, 10.8 %, 10.9 %, 13.9% for CL1, CL1*, CL2 and CL2* respectively. These values were close to clinoptilolite samples reported in the study performed by Akdeniz (1999). The differences in water content between untreated (especially CL2) and modified zeolitic material (especially CL2*) results from decomposition of carbonate.

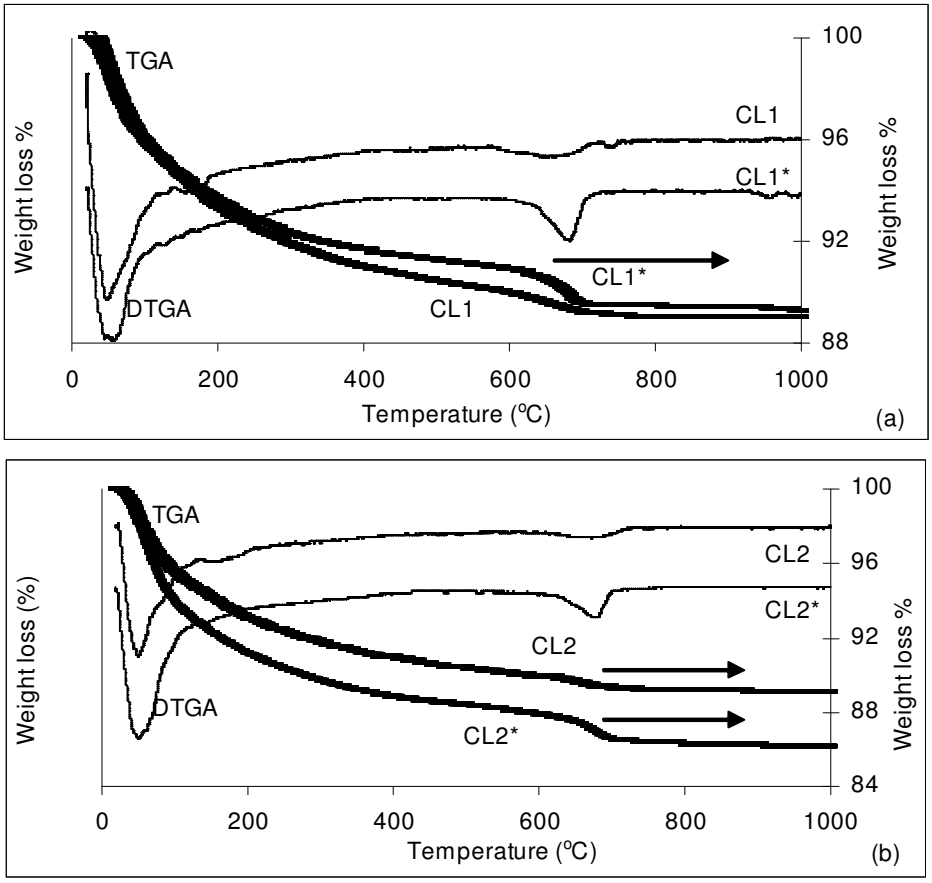

Figure 6.4. TGA and DTGA curves of the starting zeolites CL1, CL1*, CL2 and CL2*.

The surface charge of the starting zeolites in different pH values with the errors in readings (3 readings) was calculated and illustrated in Figure 6.5. Both zeolites exhibited negative charge even in acidic condition as stated in the study of Ersoy and Çelik (2002). The treatments are likely to be the causes of variation in zeta potential determination. Figure 6.5. indicates a net negative potential. The increase of suspension pH results in an increase in the negative charge of the zeolitic material. Increasing the pH to 12 brings the zeta potential to about -46 mV for untreated zeolites. This can be ascribed to either the adsorption of OH^- ions on the positively charged centers ($M\text{-}OH_2^+$ in acidic condition) of zeolites or the deprotonation of surface hydroxyl groups ($M\text{-}O^-$ in basic solutions). There was no zero point of charge between these pH values (2-12). Enrichment of zeolitic material with Na^+ caused a change in its surface charge. The negative charge was decrease for modified natural clinoptilolite in alkaline pH (pH=12) because of exchange or adsorption of Na^+ ion to the surface.

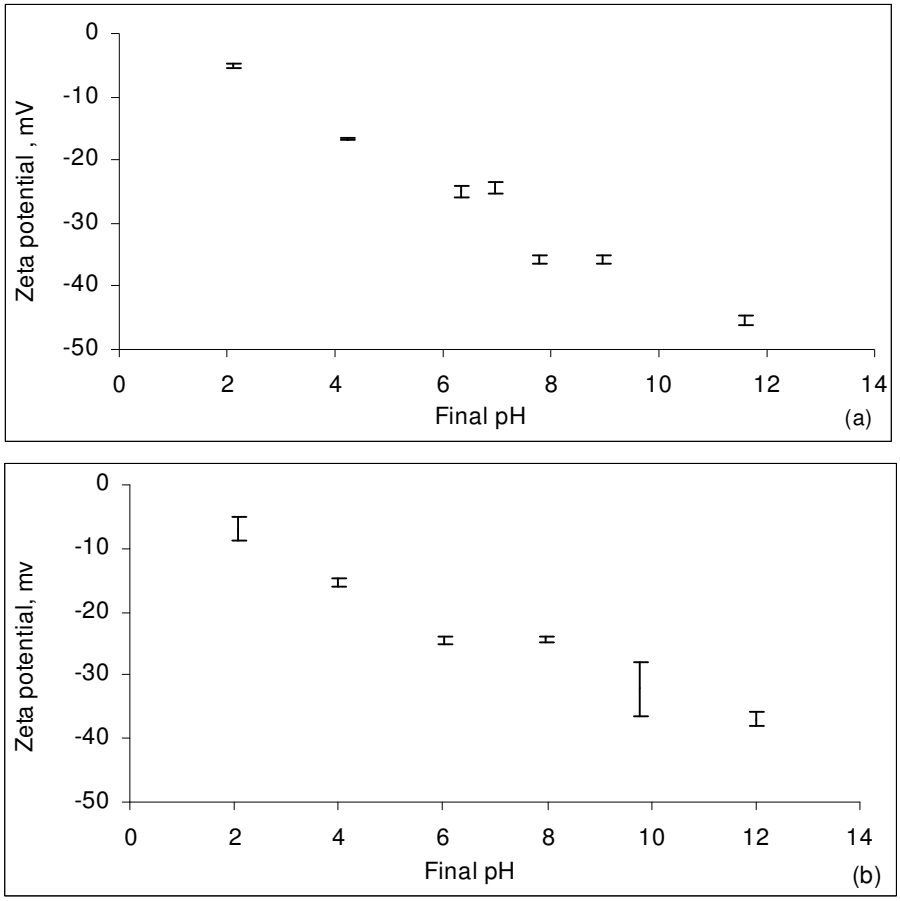

Figure 6.5. The surface charge of (a) untreated (b) modified zeolites in the 0.01 M KCl solution.

6.2. Kinetics and Equilibrium Studies in Aqueous Media

6.2.1. Aqueous Media: Hydrochloric Acid (HCl)

Figure 6.6 displays the pH evaluation of the dilute HCl solution (0.01 M). Increasing in solution pH was observed after the addition of (the first number in the codes) zeolitic material. High increases occurred when high amount of zeolite was used. The codes on the curves belong to the zeolite obtained.

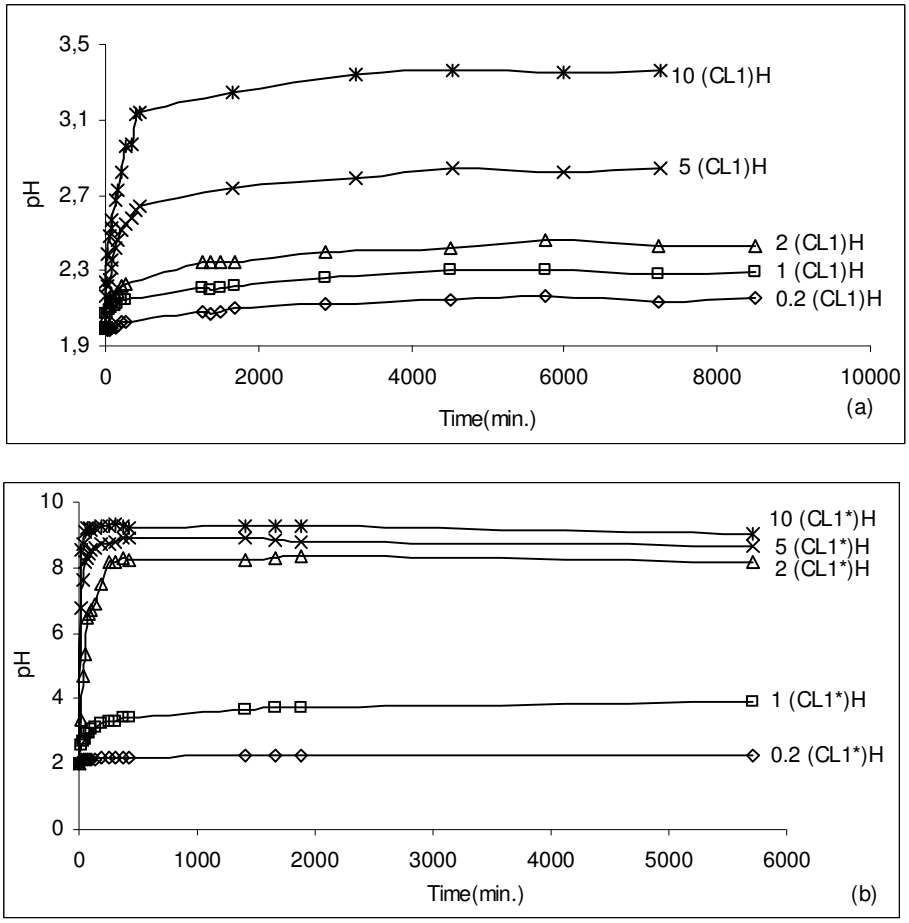

Figure 6.6. Change in pH of dilute hydrochloric acid solution after the addition of (a) as-recieved (b) modified zeolite (pH_i=2 T=37 ^oC).

A sharp increase in solution pH_e was observed when 2 %, 5 % and 10 % modified zeolites were used. CO_3^{2-} anion on the modified zeolite surface according to the equation below leads to increase OH^- concentration in the solution.

$$CO_3^{2-} + H_2O \leftrightarrow HCO_3^- + OH^-$$

In the other words the surface functional group rich in CO_3^{2-} anion is acid soluble compound and tends to gain protons from acidic solution to form soluble, slightly dissociated bicarbonate ion.

The pH value of HCl solution attained at about 6000 minute (5 days) with zeolite percentage and presented in Figure 6.7. The linear relation ship between equilibrium pH value, pHe and zeolite percentage (CL1) used was obtained for untreated zeolite

$$pH_e = 0.1224\ CL1 + 2.1686$$

On the other hand the relation ship between the pH_e and zeolite amount of modified ones (CL1*) is more complicated. The effect of zeolite amount at above 2 % was not significant while it is very effective at lower zeolite percentage. This may be explained with the presence of the same amount of total proton and hydroxide remained in solution so removal of surface complexes rich in CO_3^{2-} did not occurred at pH 8. For that reason pH_e value reached to about 8 when modified zeolite was used, but not in untreated one.

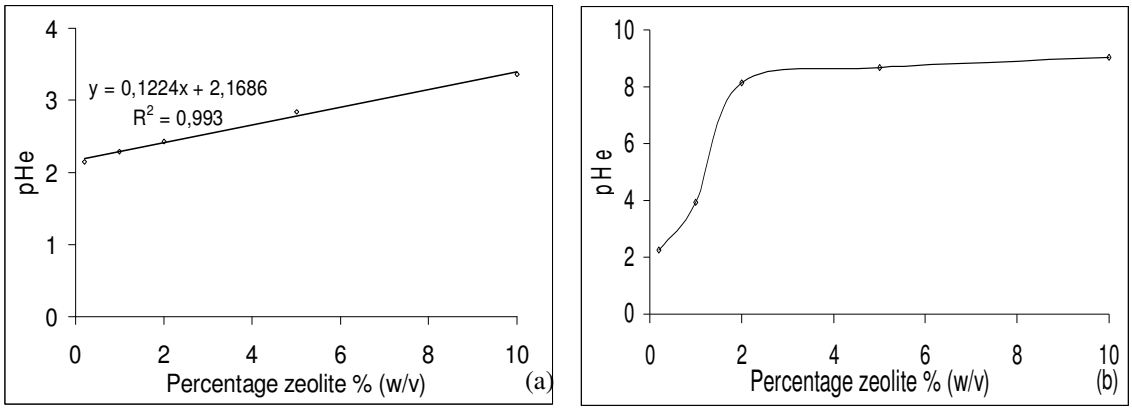

Figure 6.7. Equilibrium pH of solutions based on zeolite amount of (a) untreated (b) modified zeolites in hydrochloric acid solution system (pHi=2 T= 37 ^oC).

The proton transfer isotherms for these zeolites were obtained by using the equilibrium proton concentration in solution. The isotherm presented in the Figure 6.8. (b). is the stepwise showing the presence of the adsorption of proton on the carbonated surface. Hence different mechanisms in the proton transfer in presence of carbonated surface such as dissolution, sorption on surface complex should be taken account in this process.

For untreated zeolite, proton transfer mechanism in the acidic region can be examined in the context of three basic types of reactions: ion exchange, adsorption at surface bridging oxygen bonds (Si–OH–Al), and adsorption at surface Si–OH and Al–OH groups. The first type of adsorption reaction is associated with the exchange reaction between $H^+_{(aq)}$ and surface and near-surface cations (Na^+, Ca^{2+}, Mg^{2+}).

$[S\text{-}OM]_z + [H]_s \leftrightarrow [S\text{-}OH]_z + [M]_s$ result in increase in pH.

Zeolites may also absorb H^+ and so increasing of solution pH is observed. The third type of adsorption reaction is associated with the protonation of neutral and negative surface hydroxyl groups. In acidic solutions, zeolites may exchange some of

their exchangeable cations with H_30^+ ions, and Al can be progressively removed from the aluminosilicate framework. All types of these reactions represented below depend on the proton concentration of solution to remove the cations in clinoptilolite structure.

$$Al - OH + H^+_{(aq)} \leftrightarrow Al - OH^+_2 \leftrightarrow Al^{3+} + H_2O \quad (6.1.)$$

$$Si - O^- + H^+_{(aq)} \leftrightarrow Si - OH \quad (6.2.)$$

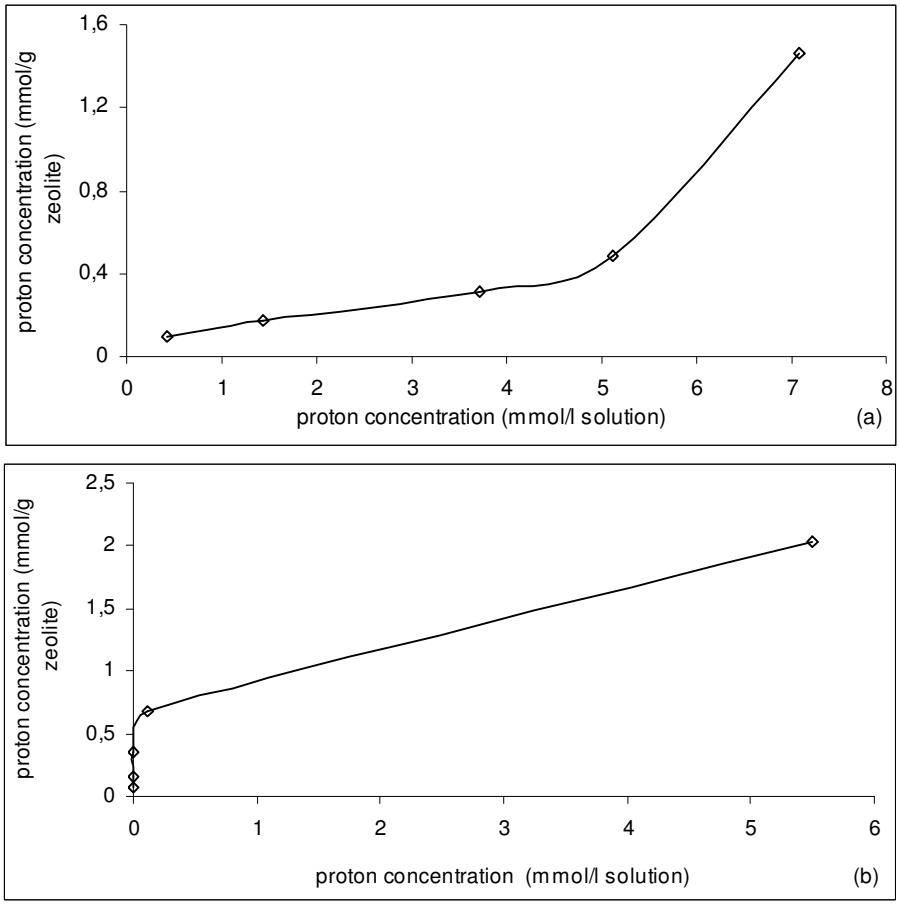

Figure 6.8. Isotherms of proton transfer for (a) untreated (b) modified zeolites.

Diffusion coefficients of proton were found from pH time data using equation 5.1. As seen from Table 6.2. the diffusion coefficients computed increases with increasing the amount of zeolite used showing the extra-particle diffusion is dominant in the proton transfer. The diffusion coefficient was close to each other for the experiment conducted with modified zeolitic material and smaller than the values for untreated ones. This is because enrichment of zeolitic mineral with Na_2CO_3 brings the excess Na^+ ions and so ion exchange or cation hydrolysis mechanism was dominant. This results also shows the overall rates of $[H^+]$ adsorption and $[HO^+_3]$ exchange

controlled by the mass transport within the zeolite pore relating the amount of crystalline material.

Table 6.2. Final pH, and proton diffusion coefficient for HCl treated samples (pH_i=2).

Zeolite	(CL1)H		(CL1*)H	
% (w/v)	Final pH	D (m^2/min)x10^{17}	Final Ph	D (m^2/min)x10^{17}
0.2	2.15	6.52	2.26	0.3
1	2.29	13.26	3.92	1.5
2	2.43	14.76	8.16	19.5
5	2.84	42.61	8.67	22.2
10	3.36	102.87	9.03	22.2

In order to analyze the interactions in zeolite-aqueous solution the amount of proton entered to the zeolite and the amount of cations removed from zeolite was calculated and presented in Table 6.3.

Table 6.3. **:** Equilibrium cation [M]e, and hydrogen [H]e amount in HCl solution ($[H]_0$=1 mmol).

Codes	Zeolite % w/v	$[H]_e$ (mmol)	$[M]_e$ (meq)	($[H]_0$-[H]e)/ [H]o)*100
0.2 (CL1)H	0.2	0.71	0.24	29
1 (CL1)H	1	0.51	0.60	49
2 (CL1)H	2	0.37	0.84	63
5 (CL1)H	5	0.14	1.22	86
10 (CL1)H	10	0.04	0.99	96
0.2 (CL1*)H	0.2	0.59	0.39	41
1 (CL1*)H	1	0.06	0.74	94
2 (CL1*)H	2	0.05	0.84	95
5 (CL1*)H	5	0.05	1.20	95
10 (CL1*)H	10	0.05	1.52	95

The ratio of transferred proton to the initial proton amount (available) in the solution (the last column on the Table) is expected to be 100 % when the all proton is consumed. This ratio increases with increasing zeolite amount used in solution. 10 % untreated zeolite consumed 96 % of proton available in solution while 1 % of modified zeolite was enough to consume 94 % of the proton. The exchanged amount for cation and proton was used to calculate the cation and proton amount as shown in Figure 6.9.

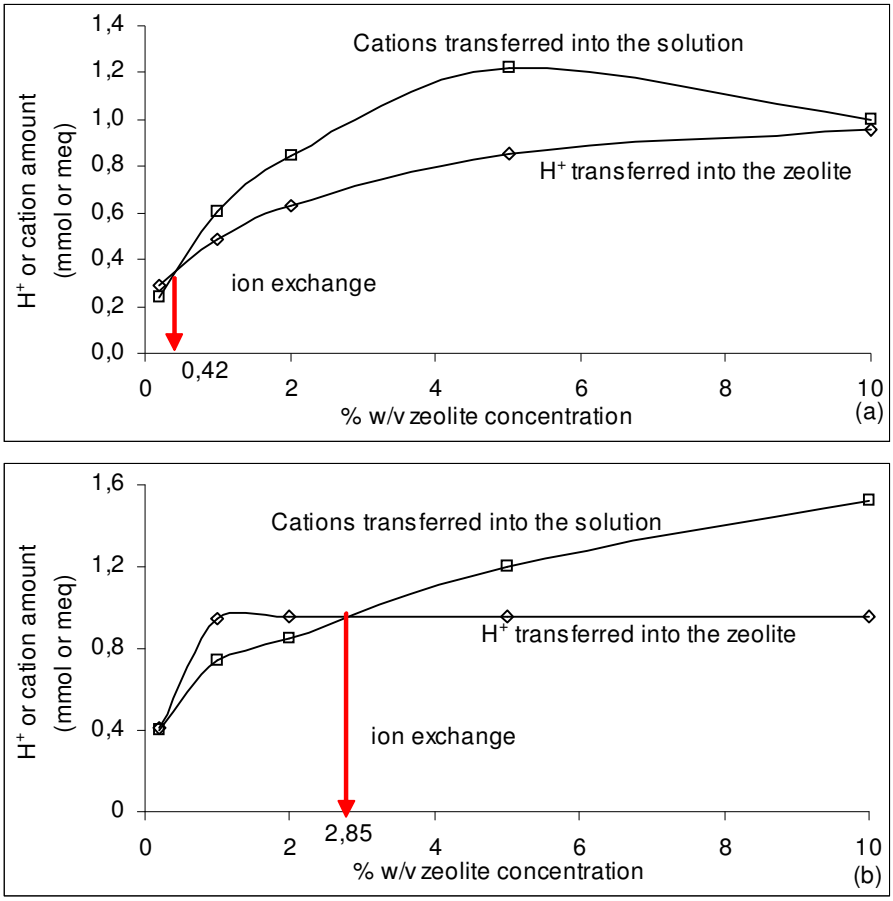

Figure 6.9. Evaluation of exchange mechanism between (a) untreated (b) modified zeolite in dilute hydrochloric acid solutions.

The curves related to the cation transferred into solution crossed over the curve related to the proton transferred into solution at 0.42 % zeolite amount and 2.85 zeolite amount when untreated and modified zeolite was used. At low zeolite concentration, proton is sorbed by untreated zeolite to protonate the surface.

(protonated surface) $M-OH_2^+ \xleftrightarrow{H^+} M-OH$ (neutral surface)

The cation release is started with increasing zeolite amount used. When 96 % of proton in solution was transferred to zeolite, the transferred is accomplished. The modified zeolite sorbed high amount of proton initially to dissolve some unstable complexes. These unstable complexes then dissolved to make the solution rich in bicarbonate. So high zeolite content (> 2%) made the acidic solution base at equilibrium. For all zeolite content of solution, the cation in solution increased due to the hydrolysis of cation in basic media.

$$[\text{S-OM}]_z + H_2O \leftrightarrow [\text{S-OH}]z + [\text{MOH}]_s$$

The chemical composition of starting zeolites and after treatment with HCl was calculated and presented in Table 6.4. It is clear that the amount of cations transferred to the solution is mostly Na^+ ions. Because sodium and calcium ions are the weakest bound and located in larger channels in zeolite structure while potassium and magnesium have stronger bound with zeolite lattice. The cation content of HCl treated zeolites increased with increasing zeolite amount (Table 6.4.). The precipitation of cations as metal hydroxide at near neutral or basic solution pH is the reason for this increasing.

Table 6.4. Chemical composition of starting and HCl treated zeolites (mmol/g).

Codes	Na	K	Ca	Mg	Fe	Al	Si
CL1	0.23	0.70	0.32	0.46	0.28	2.99	12.05
0.2 (CL1)H	0.09	0.54	0.06	0.27	0.27	2.62	11.64
1 (CL1)H	0.13	0.64	0.21	0.35	0.28	2.93	11.86
2 (CL1)H	0.15	0.66	0.25	0.38	0.28	2.98	11.95
5 (CL1)H	0.18	0.68	0.28	0.42	0.28	2.98	12.01
10 (CL1)H	0.21	0.69	0.28	0.44	0.28	2.99	12.03
CL1*	1.18	0.60	0.23	0.40	0.25	2.47	9.97
0.2 (CL1*)H	0.44	0.48	0.00	0.23	0.24	2.34	9.76
1 (CL1*)H	0.68	0.58	0.19	0.33	0.25	2.46	9.89
2 (CL1*)H	0.81	0.59	0.22	0.39	0.25	2.46	9.90
5 (CL1*)H	0.96	0.59	0.22	0.39	0.25	2.47	9.93
10 (CL1*)H	1.05	0.59	0.23	0.39	0.25	2.47	9.95

The increase in cation concentrations of acid solution and rapid adsorption of H^+ onto the negatively charged clinoptilolite surface (protonation) leads to decrease in proton concentration in solution. Surface protonation tends to increase the dissolution, because it leads to highly polarized interatomic bonds in the immediate proximity of the surface central ions and thus facilitates the detachment of a cationic surface group into the solution. The formation of surface complexes explained in the reaction 6.1. increases Al dissolution and consequently increases Al^{3+} hydrolysis, which takes place when Al^{3+} species come into the solution.

Dissolution of Al and Si atoms from zeolite lattice were monitored. The dissolution is higher for the smallest zeolite amount used due to strong interaction of solid-solution system as presented in Table 6.5. Dissolution of Al and Si from zeolite lattice decreased was not observed with increasing the zeolite amount and low for

modified zeolites when compared with untreated ones. As seen from Table 6.5. TEC is related to dissolved Al and Si for untreated and modified zeolites.

Table 6.5. Dissolved Al (D_{Al} %) and Si (D_{Si} %) atoms from zeolite lattice in HCl solution.

Code	Zeolite (% w/v)	D_{Al} (%)	D_{Si} (%)	TEC (meq/g)
CL1	0.0	0.00	0.00	2.49
0.2 (CL1)H	0.2	13.33	3.86	1.29
1 (CL1)H	1	2.22	1.78	1.89
2 (CL1)H	2	0.52	0.91	2.07
5 (CL1)H	5	0.08	0.40	2.25
10 (CL1)H	10	0.03	0.21	2.39
CL1*	0.0	0.00	0.00	3.06
0.2 (CL1*)H	0.2	5.02	2.11	1.11
1 (CL1*)H	1	0.04	0.84	2.32
2 (CL1*)H	2	0.02	0.73	2.64
5 (CL1*)H	5	0.03	0.49	2.82
10 (CL1*)H	10	0.03	0.21	2.91

Figure 6.10 shows dissolution of Al and Si as well as the amount of transferred cation in to solution depending on the ratio of available proton to cation. When the ratio is high both dissolved Si, Al and amount of transferred cation is high indicating the strong interaction of proton.

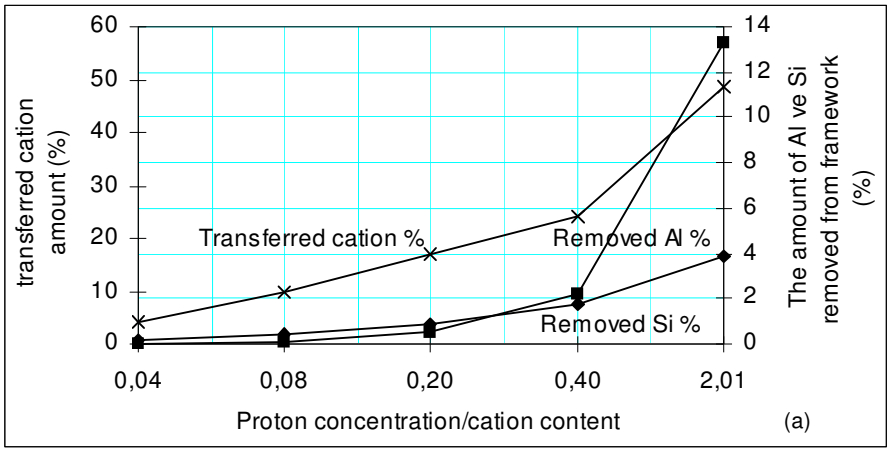

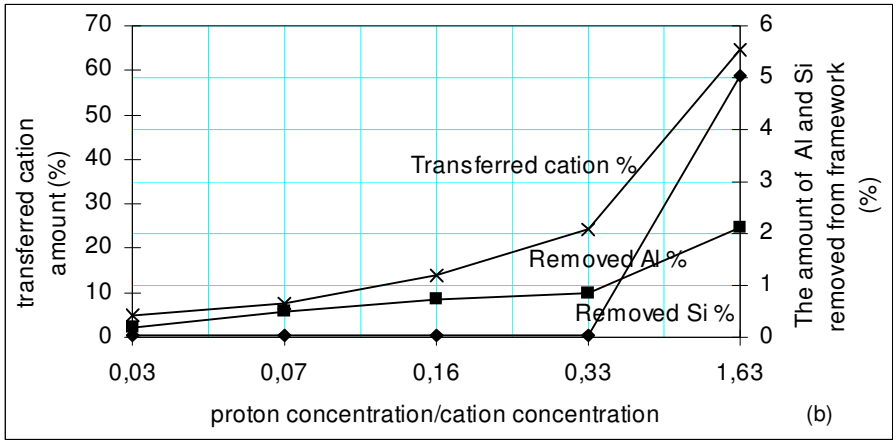

Figure 6.10. The dissolved Si,Al and cations amount in hydrochloric acid solution when the starting zeolite in (a) as-received (b) modified form.

6.2.2. Aqueous Media: Synthetic Gastric Juice (SGJ)

The chemical behavior of as-received and modified zeolite in the presence of SGJ was also studied. pH and zeolite amount are effective on pepsin activity (decrease in UV absorbance of the solution). The pH of the solution including 0.4 % pepsin was adjusted 1.5, 2, 2.5 and 3 by using HCl to see the effect of pH on pepsin activity (Figure 6.11.). It was observed that the activity of pepsin decreased with increasing pH (>2). So the chemical behavior of zeolite was investigated at pH=2. The effect of zeolite amount on the pepsin activity was tabulated in Table 6.6.

Table 6.6. The effect zeolite amount and solution pH on the pepsin activity in simulated gastric juice (pH_i=2), #: equilibrium.

Codes	Final pH	Absorbance (at 275nm)	Activity %	Decrease in activity
% 0,4 Pepsin	2	0,569	100	0
0.02 (CL2*)P	2,18	0,479	84	14
0.5 (CL2*)P #	2,88	0,395	69	18
1 (CL2*)P	5,64	0,41	72	nd
5 (CL2)P	2,7	0,13	22	69

#: equilibrium, nd: not determined.

Zeolite amount is very effective parameter for pepsin activity. Decrease in activity was very low for the concentration of 0.02 % and 0.5 % (14 % and 18 % respectively). However for the zeolite concentration of 5 % decrease in activity was

very high (69 %) as shown in Figure 6.11. Decrease in pepsin activity was not determined for the zeolite concentration of 1 %. Because in this concentration of modified zeolite the pH of the solution reached to 5.64 which was very high for stomach acidity.

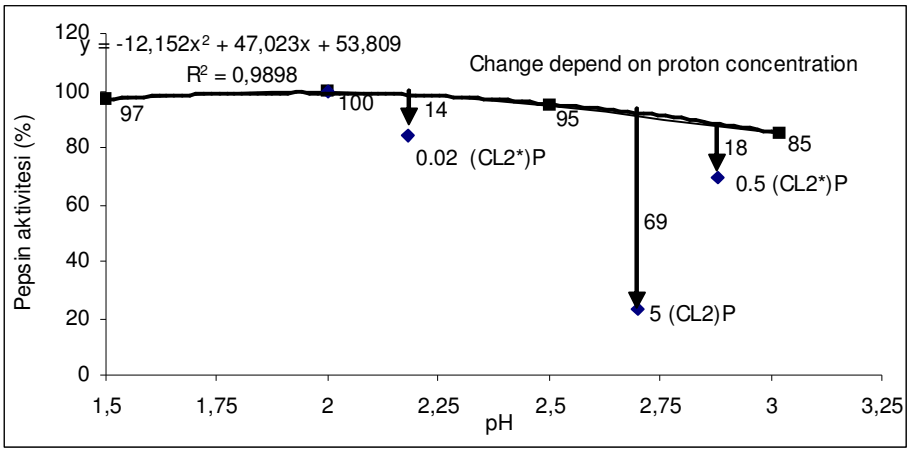

Figure 6.11. The effect of zeolite (points) and solution pH (line) on the pepsin activity in simulated gastric juice.

The neutralizing capacity of modified zeolite was very high when compared 1(CL2*)P and 5(CL2)P (2 hours experiments) as shown in Table 6.6. The temporal increase of the pH value in suspensions is partly a result of the exchange of H^+ and partly of the binding of proton to the Lewis basic sites. The exchange process occurs between solutions protons and exchangeable cations in clinoptilolite lattice. Exchangeability depends on zeolite concentration, and the composition and exchangeability of cations in the zeolite structure. Table 6.7. shows the chemical composition of starting and SGJ treated zeolites. It is apparent that Na^+ ions are most easily exchanged cation because of weakest bonds and modified in the other words Na^+ reach zeolite was higher neutralizing capacity. Carbonate ions also affect the increasing mechanism by catching the proton from the solution.

Table 6.7. Chemical composition of starting and SGJ treated zeolites (mmol/g).

Codes	Na	K	Ca	Mg	Fe	Al	Si
CL2	0.30	0.77	0.39	0.46	0.29	3.1	11.84
5 (CL2)P	0.12	0.69	0.19	0.28	0.28	3.09	11.80
CL2*	1.55	0.65	0.38	0.41	0.26	2.83	10.79
0.5 (CL2*)P	1.17	0.63	0.34	0.32	0.25	2.82	10.77
1 (CL2*)P	0.91	0.63	0.32	0.35	0.26	2.83	10.74

The amount of 0.5 g modified zeolite was sufficient in order to neutralize the SGJ as shown in Figure 6.12. This is because there was no significant decrease in pepsin activity and the solution pH was near optimum value which is between 2.9 and 3.1.

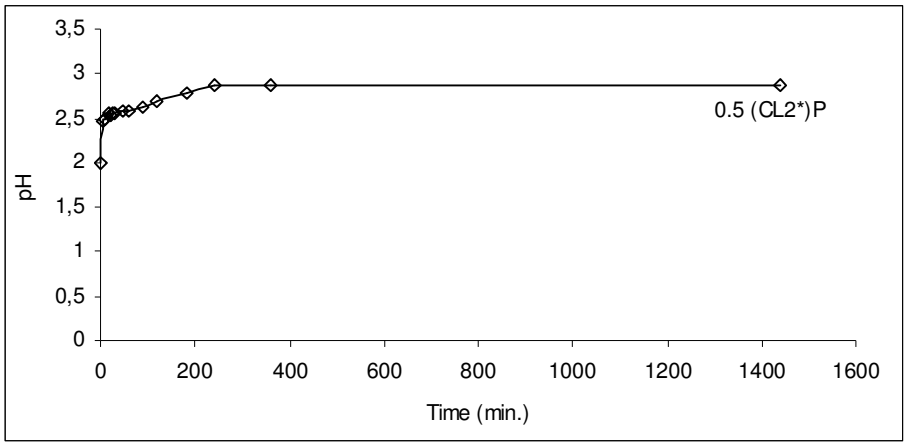

Figure 6.12. Evaluation of synthetic gastric juice solution pH with time (Zeolite: 0.5%).

The ratio of the amount of protons transferred to the zeolite and the amount of proton available initially in solution was calculated in order to analyze the interactions between zeolite and SGJ (Table 6.8.). From the ratio (the last column in the Table) it was understood that the transferred proton present initially in the solution is depleted and could not balance the cations. In the suspension containing the zeolite of 0.5 and 1 % , mainly proton was sorbed by increasing amount of zeolite. For modified ones dissolution mechanism was dominant ([M]e>([H]e-[H]o)). This behavior of zeolite is the same as in HCl solution.

Table 6.8. Equilibrium cation [M]e, and hydrogen [H]e amount in SGJ solution ($[H]_0$=1mmol).

Codes	Zeolite % w/v	$[H]_e$ (mmol)	$[M]_e$ (meq)	$([H]_0-[H]e)/ [H]o)*100$
0.5 (CL2*)P	**0.5**	0.13	0.66	87
1 (CL2*)P	**1**	0.01	0.90	99
5 (CL2)P	**5**	0.20	1.02	80

Removal of Al and Si atoms from natural clinoptilolite lattice were tabulated in Table 6.9. Their removal was very low level.

Table 6.9. Dissolved Al (D_{Al} %) and Si (D_{Si} %) atoms from zeolite lattice in SGJ solution.

Code	D_{Al} (%)	D_{Si} (%)	TEC (meq/g)
CL2	nd	nd	2.77
CL2*	nd	nd	3.79
0.5 (CL2*)P	0.18	0.18	2.47
1 (CL2*)P	0.01	0.5	2.89
5 (CL2)P	0.02	0.03	2.57

nd: not detected.

6.2.3. Aqueous Media: Acetic Acid ($C_2H_4O_2$)

Figure 6.13. shows the change in pH of the acetic acid (weak electrolyte) solution with time in the presence of zeolite (5%w/v).

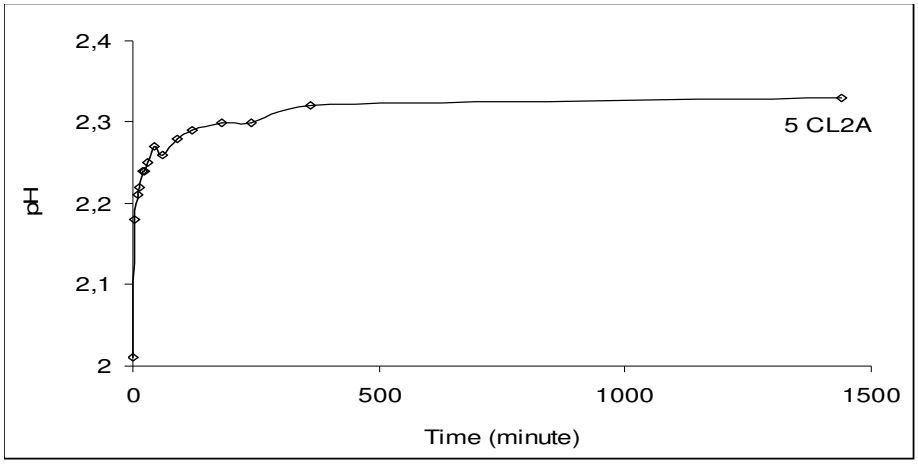

Figure 6.13. Change in acetic acid solution pH with time (pHi=2, T=37 ^oC).

Zeolite increased the solution pH to 2.31 (from 2) in 500 min (8.3 h). Possible mechanism responsible for increasing in solution pH can be as follow;

(a) Ion exchange $(\equiv S\text{-}OM)_z+(H^+ + CH_3COO)_s \leftrightarrow (\equiv SOH)_z+(M^+ + CH_3COO^-)_s$

(b) Sorption $(\equiv S\text{-}OH)_z+(H^+ + CH_3COO^-)_s \leftrightarrow (\equiv S\text{-}OH^+_2)_z+(CH_3COO^-)_s$

53 % of initial proton was only used to transfer cation to solution. The transferred cation form zeolite (0.76 meq) was higher than proton transferred (0.53 mmol) from the acetic acid solution. The most transferred cation is Na^+ ion as shown in Table 6.10.

Table 6.10. Chemical composition of starting and $C_2H_4O_2$ treated zeolites (mmol/g).

Codes	Na	K	Ca	Mg	Fe	Al	Si
CL2	0.30	0.77	0.39	0.46	0.29	3.1	11.84
5 (CL2)A	0.28	0.76	0.36	0.43	0.28	3.09	11.82

The ratio of the cation transferred to proton transferred (1.23) is higher than 1. This shows that hydrolysis of cation occurred in acidic media. The adsorption on the surface to cause the inner, outer sphere complex or precipitation is not possible in the acetic acid solution. The dissolved Al and Si percent was low (0.19% and 0.23 % respectively) and TEC of the zeolite is not significantly changed (TEC: 2.77meq/g and 2.62 meq/g for untreated and acetic acid treated zeolite). Diffusion coefficient of proton to zeolite is calculated and found as 7.7×10^{-17} m^2/s.

6.2.4. Aqueous Media: Lactic Acid ($C_3H_6O_3$)

Chemical behavior of the untreated and modified zeolites (5% w/v) in lactic acid solution was investigated by varying the initial pH of the solution and presented in Figure 6.14. The reason to keep solution initial pH at 2, 4 and 5.5 is to check the attainability of the lactic acid fermentation pH (pH=5-5.5). Figure 6.14. shows the change in pH of the Lactic acid with addition of zeolite 5 % (w/v). As seen from the Figure, the pH of the solution is not changed considerably with time and reached equilibrium in very short time (9 min.). The addition of the zeolite to the lactic acid solution at pH 4 and 5.5 resulted in increase in pH to 11 in very short period of time (4 min.) and reached to equilibrium at about pH 10. This pH value is not acceptable for lactic acid fermentation media.

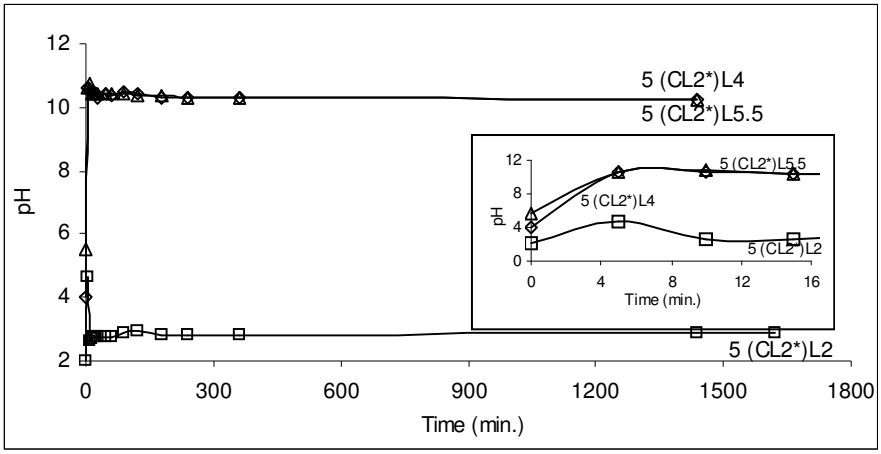

Figure 6.14. Change in Lactic acid solution pH with time.

In the case of initial pH 2, a rapid increase in pH takes place in the first 4 min, while a slow decrease occurred afterwards reaching a plateau at about pH 3. Table 6.11. shows the effect of the initial pH on the proton ($[H]_o$-$[H]_e$) and the cation transferred ($[M]_o$-$[M]_e$) during the Lactic acid treatment. Initial proton concentration is effective on the exchanged amount of cation. 83 % of the proton present in the solution was used by adding the modified zeolite at pH 2. However the proton in the solution was consumed for higher solution pH. Similar behavior was observed when untreated zeolite was used.

Table 6.11. Proton ($[H]_o$-$[H]_e$) and the cation exchanged ($[M]_o$-$[M]_e$) during the Lactic acid treatment. Zeolite percentage: 5%(w/v). $[M_o]_z$ = 13.90 and 18.95 meq for untreated and modified zeolite.

Code	**pH_i**	**$[H]_o$ (mmol)**	**($[H]_o$-$[H]_e$) (mmol)**	**($[M]_o$-$[M]_e$) (meq)**
5 (CL2)L4	4	0.01	0.01	0.07
5 (CL2*)L2	2	1	0.83	3.90
5 (CL2*)L4	4	0.01	0.01	2.15
5 (CL2*)L5.5	5.5	0.0003	0.0003	2.09

Cationic sites are not balanced by proton indicating not only ion exchange but also hydrolysis of cations or complexation mechanisms by means of sorption accomplished in Lactic acid solution.

The exchanged cations and proton are related to their initial concentration in solution. Dissolution of Al and Si was low level (Table 6.12.). A decrease in TEC is the most in the zeolite treated at pH 2 due to presence of sufficient amount of proton in the solution to transfer the cation.

Table 6.12. Dissolved Al (D_{Al} %) and Si (D_{Si} %) atoms from zeolite lattice in $C_3H_6O_3$ solution.

Code	**D_{Al} (%)**	**D_{Si} (%)**	**TEC (meq/g)**
CL2	0.00	0.00	2.77
5 (CL2)L4	0.14	0.19	2.76
CL2*	0.00	0.00	3.79
5 (CL2*)L2	0.85	0.68	3.01
5 (CL2*)L4	0.32	0.95	3.36
5 (CL2*)L5.5	0.31	0.90	3.37

The dissolved aluminum amount is higher for modified zeolite when 5 (CL2)L4 and 5 (CL2*)L4 is compared to each other. Figure 6.15. displays the effect of the modification on solution pH when 5% zeolite put into the solution (pH_i= 4). Significant increase in solution pH to 7 and 10 shows all the protons in solution was consumed by used zeolites.

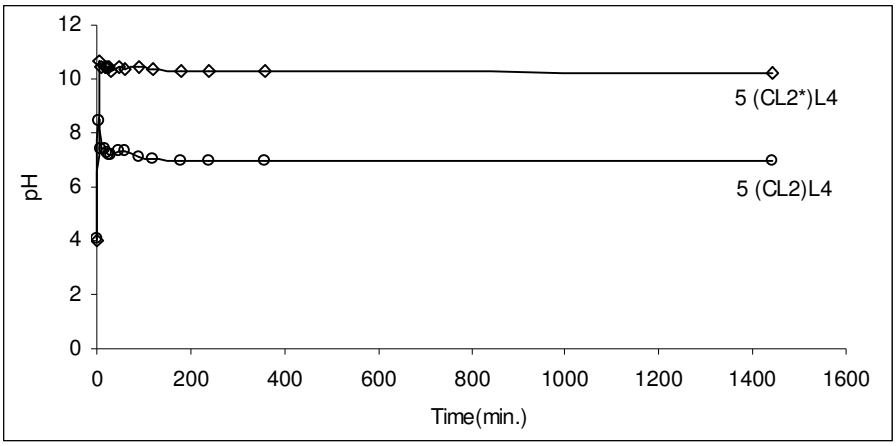

Figure 6.15. Effect of pretreatment on Lactic acid solution pH (pHi=4).

Lactic acid, a weak electrolyte can not easily ionize in the aqueous solution. Possible mechanisms between lactic acid and untreated zeolite are given below:

(a)Ion exchange $(\equiv S\text{-}OM)_z+(H^+ + CH_3CHOHCOO^-)_s \leftrightarrow (\equiv SOH)_z+(M^+ + CH_3CHOHCOO^-)_s$

(b)Sorption $(\equiv S\text{-}OH)_z+(H^+ + CH_3CHOHCOO^-)_s \leftrightarrow (\equiv S\text{-}OH^+_2)_z+(CH_3CHOHCOO^-)_s$

The protonated surface ($\equiv S\text{-}OH^+_2$) is obtained into lactic acid solution as in the other acid solutions. In the mechanism (a) exchanged cation amount increases and not effective significantly on pH increase (proton concentration decrease). In the second mechanism, mechanism (b), the formation of protonated surface by sorption causes

considerable decrease in proton concentration. By means of sorption the inner and/or outer surface complexation, precipitation (as sodium or calcium acetate) can occur. The modification made the surface rich in sodium. Therefore exchanged sodium was high for modified zeolite as shown in Table 6.13. The surface was rich also with carbonate which is soluble in weak acid solution.

Table 6.13. Chemical composition of starting and $C_3H_6O_3$ treated zeolites (mmol/g).

Codes	Na	K	Ca	Mg	Fe	Al	Si
CL2	0.30	0.77	0.39	0.46	0.29	3.10	11.84
5 (CL2)L4	0.29	0.76	0.38	0.45	0.28	3.09	11.82
CL2*	1.55	0.65	0.38	0.41	0.26	2.83	10.79
5 (CL2*)L2	1.09	0.63	0.31	0.33	0.25	2.81	10.72
5 (CL2*)L4	1.22	0.64	0.37	0.37	0.25	2.82	10.69
5 (CL2*)L5.5	1.23	0.64	0.37	0.37	0.25	2.82	10.70

6.2.5. Aqueous Media: Sodium Hydroxide (NaOH)

Figure 6.16. shows the change in pH of the basic solution with addition of natural zeolite. The more amount of zeolite used the more decrease in solution pH was observed for 400 min (the small figure). However this order was changed in the following time period.

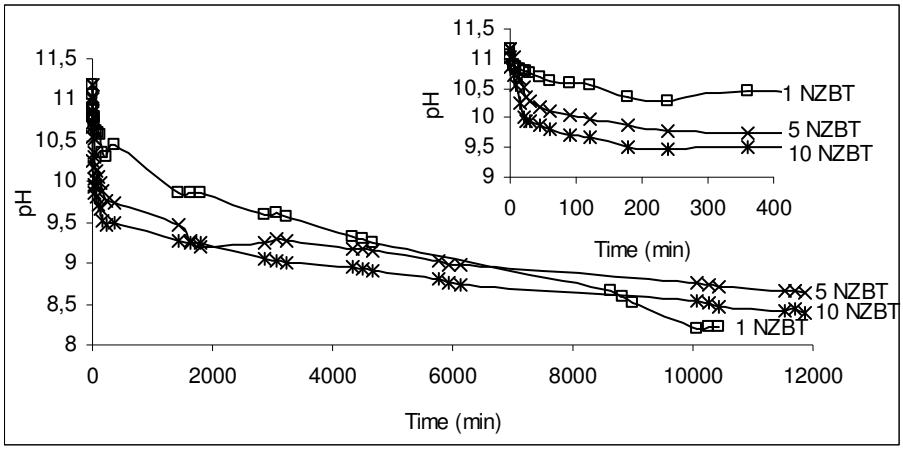

Figure 6.16. Change in pH of sodium hydroxide solution (0.00148 M) with time (pH_i=11.17 T=27 ^oC).

Zeolite amount was effective in decrease rate of the solution while not effective on equilibrium pH of the solutions (it is between 8.1-8.6). The decrease in the solution pH with the addition of zeolite can be expressed by the reaction of OH^- with zeolite surface (S).

$$[\equiv S\text{-}OH] + OH^- \leftrightarrow [\equiv S\text{-}O^-] + H_2O$$

$[\equiv S\text{-}OH]$ and $[\equiv S\text{-}O^-]$ represent the neutral and deprotonated surface respectively.

This reaction acquires an overall negative charge, due to the increasing predominance of both $Si–O^-$ and $Al–O^-$ groups and has two consequences:

(i) The decrease in solution pH and

(ii) The formation of more available negative charge on the zeolite framework.

To maintain charge neutrality, the produced negative charge is counterbalanced by solution cations (mainly Na) through complexion reactions; outer and inner-sphere. The adsorption of OH on the S-OH sites result in the formation of $S\text{-}OH^-$ site that is the initial phase for outer-sphere complexion which involves the ion-exchange reactions between metal ions (Na^+) and surface counterbalance cations. Inner-sphere complexion leads to more stable surface groups due to the formation of covalent bonds. Hydrogen cations are released as products and the process causes a total decrease in solution pH. The following reactions represent these two mechanisms for Na^+ ions:

Inner-sphere complex: slow and irreversible: $S\text{-}OH + Na^+ \leftrightarrow S\text{-}ONa + H^+$

Outer-sphere complex: rapid and reversible: $(S\text{-}O^-)_2 + Na^+ \leftrightarrow (S\text{-}O^-)_2 \ldots Na^+$

The reason for higher decrease in solution pH, when 1 % of zeolite used can be the formation of inner sphere complex and so H^+ ion concentration was increased. The differences between initial and final concentration of Na^+ ions is lower for 5 % of zeolite as shown in Table 6.14. explaining that outer-sphere complexion mechanism was dominant and the product of hydrogen ions are less. This is because decreasing of pH was lower than the other samples.

In order to analyze the interactions between zeolite and NaOH solution, the amount of hydroxide entered to the zeolite and the cations released from zeolite calculated and presented in Figure 6.17. This ratio cation to hydroxide transfer is higher than 1 for all zeolite amounts used pointing out that released amount from zeolite is higher than the transferred amount from solution.

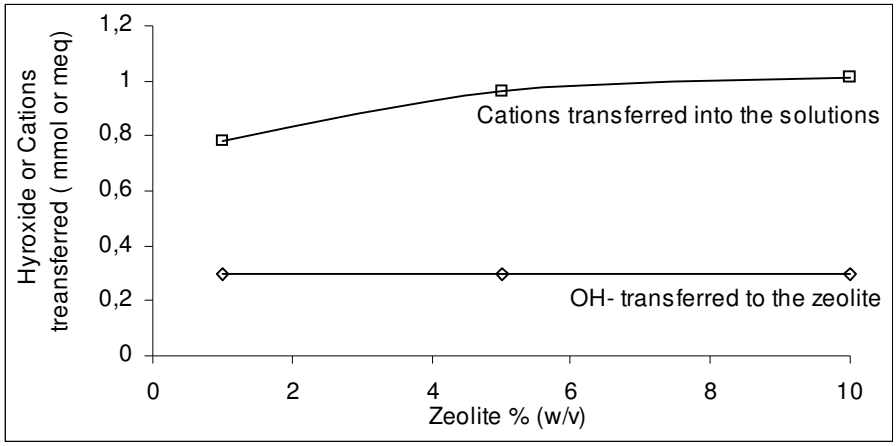

Figure 6.17. Evaluation of exchange mechanism between untreated zeolite and sodium hydroxide solution.

As shown in Table 6.14. the OH^- ions was completely adsorbed on the zeolite structure.

Table 6.14. Equilibrium cation [M]e, hydroxide and sodium amount in NaOH solution ($[OH^+]_0$=0.296 mmol, $[H]_0=1.4*10^{-9}$mmol, $[Na^+]_0$=0,296 mmol.

Zeolite % w/v	**$[M]_e$ (meq)**	**$[Na^+]_e$ (meq)**	**$[OH]_e$ (mmol) (10^{-4})**	**$[H]_e$ (mmol) (10^{-7})**
1	0,61	0,17	2.4	0.16
5	0,78	0,18	8.5	4.7
10	0,84	0,16	4.9	8.1

Transferred cations amount in alkali solution was determined as presented in Table 6.15. The Na^+ ion was mostly removed cation as in the other solutions.

Table 6.15. Chemical composition of starting and NaOH treated zeolites (mmol/g).

Codes	**Na**	**K**	**Ca**	**Mg**	**Fe**	**Al**	**Si**
CL2	0.30	0.77	0.39	0.46	0.29	3.1	11.84
1 (CL2)S	0.22	0.75	0.38	0.33	0.29	3.0	11.79
5 (CL2)S	0.28	0.76	0.38	0.43	0.29	3.0	11.82
10 (CL2)S	0.29	0.76	0.38	0.44	0.29	3.0	11.83

In the alkali solution, removal of Si and Al atom from zeolite was very low level. Dissolved percent of Al and Si atoms from natural clinoptilolite lattice were presented in Table 6.16. Under alkali experimental conditions the lack of solution $[H^+]$

caused to the inhibition of Al dissolution. Si dissolution is higher when compared with Al dissolution at basic pH, because the Si–O bonds are polarized and weakened by the presence of the charged surface species Si–O^-. This ultimately leads to the detachment of the silicon atom.

Table 6.16. Dissolved Al (D_{Al} %) and Si (D_{Si} %) atoms from zeolite lattice in NAOH solution

Code	D_{Al} (%)	D_{Si} (%)	TEC (meq/g)
CL2	0.00	0.00	2,78
1 (CL2)S	0.04	0,51	2.16
5 (CL2)S	0.02	0,16	2.62
10 (CL2)S	0.04	0,11	2.70

Diffusion coefficient of hydroxide from the solution as presented increased by increasing the zeolite amount used in the solution in Table 6.17.

Table 6.17. Final pH during the hydroxide diffusion in untreated zeolite.

% (w/v)	Final pH	D (m^2/min)x10^{16}
1	8.1	3.36
5	8.63	10.8
10	8.39	17.9

6.3. Characterization of The Zeolites

Whether the zeolite phase is effected or not from treatments was detected by using X-Ray diffraction, Thermal Analysis, FTIR methods and Zeta Potential measurements.

6.3.1. XRD Studies

From the X-Ray diffraction pattern (Figure 6.18.) the zeolites has peaks at 9.88°, 22.49° indicating clinoptilolite crystals with impurity of quartz (26.67° =2θ). Decrease in clinoptilolite characteristic peaks for 0.2 and 1 % HCl treated zeolite content due to

the partially dissolution of Al and Si (D_{Al}=13.33%, 2.22 and D_{Si}=3.86%, 1.78% respectively). On the other hand increase in the characteristic peaks for higher zeolite content than 1 % indicates that dilute HCl solution purified the clinoptilolite rich tuff.

The formation of the new peaks at 38.51°, 27.99°, and 26.99° 2θ were attributed to sodium aluminum hydroxide (S), albite (A) ($Na(AlSi_3O_8)$) and α-quartz (Q). These outer surface complexes were obtained in high content of zeolite usage (2% and 10%).

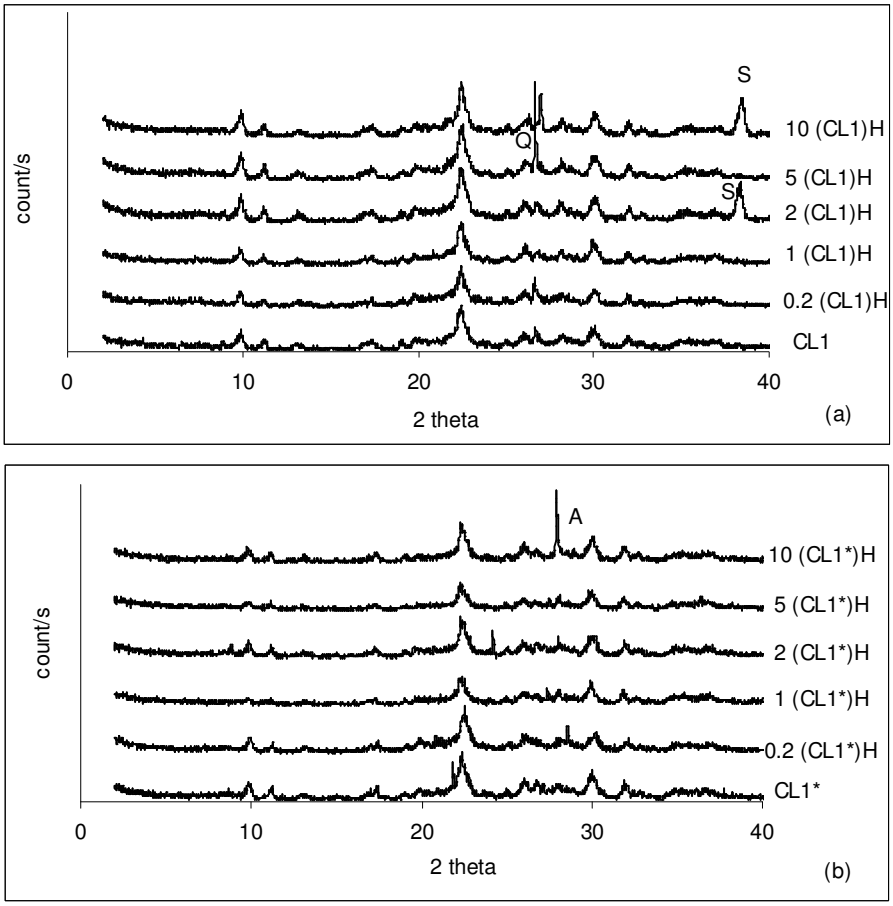

Figure 6.18. X-Ray diffraction patterns of the hydrochloric acid treated zeolites. Starting zeolite: (a) untreated zeolite, (b) modified zeolite.

The intensity of the X-Ray diffraction peaks of the zeolites was decreased after the interaction with synthetic gastric juice as displayed in Figure 6.19. The characteristic peak at 9.8° 2θ disappeared in the experiment conducted with the zeolite concentration of 0.5 %. High interaction of zeolite with aqueous solution is the reason for this disappearance.

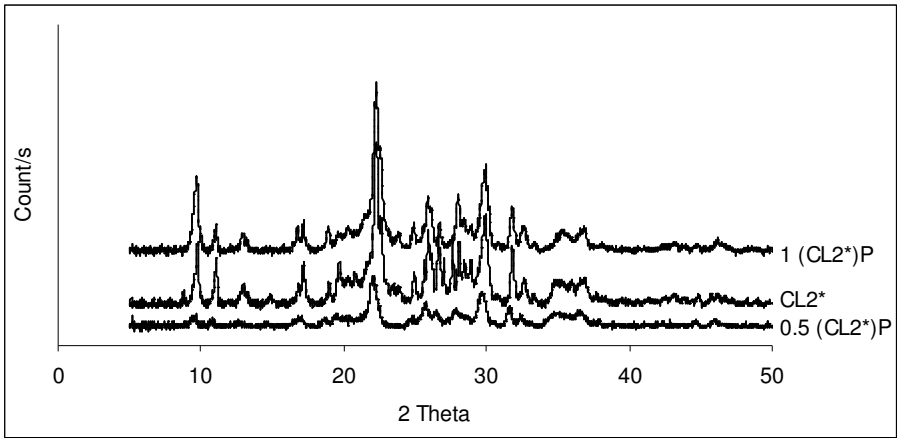

Figure 6.19. X-Ray diffraction pattern of modified and synthetic gastric juice treated zeolites.

On the other hand, the crystal structure as shown in Figure 6.20. is being evident with keeping it into SGJ solution.

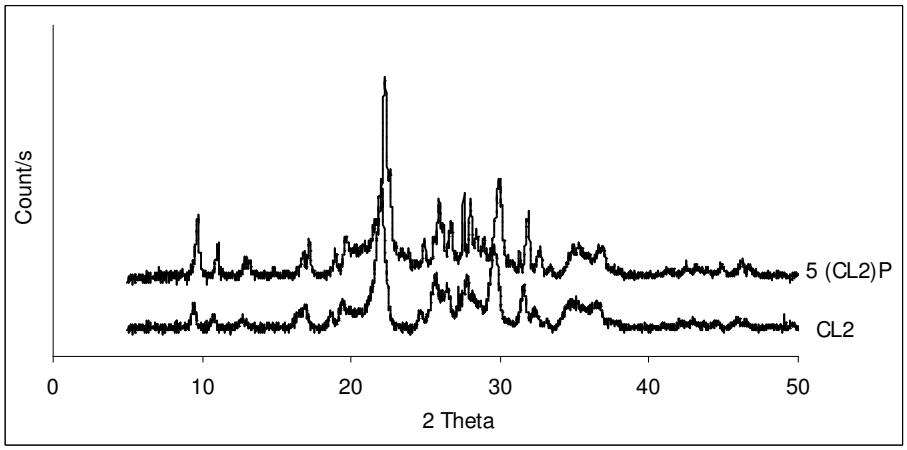

Figure 6.20. X-Ray diffraction pattern of untreated and synthetic gastric juice treated zeolites.

The comparison of the zeolite obtained with its starting zeolite shows that the crystal surface [020] observed (9.8^{o} 2θ) decreased with acetic acid treatment (Figure 6.21).

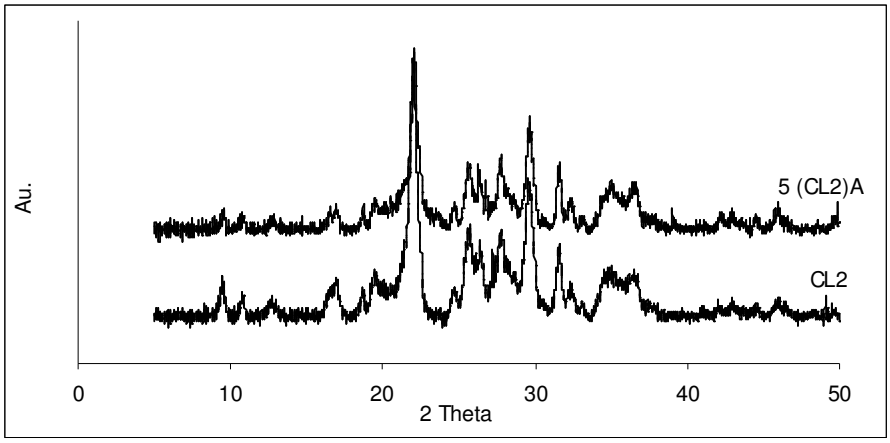

Figure 6.21. X-Ray diffraction pattern of the untreated and acetic acid treated zeolite.

Figure 6.22. displays X-ray diffraction patterns of the Lactic acid treated zeolites. The starting zeolites are as-recieved and modified in Figure 6.22.(a) and (b) respectively.

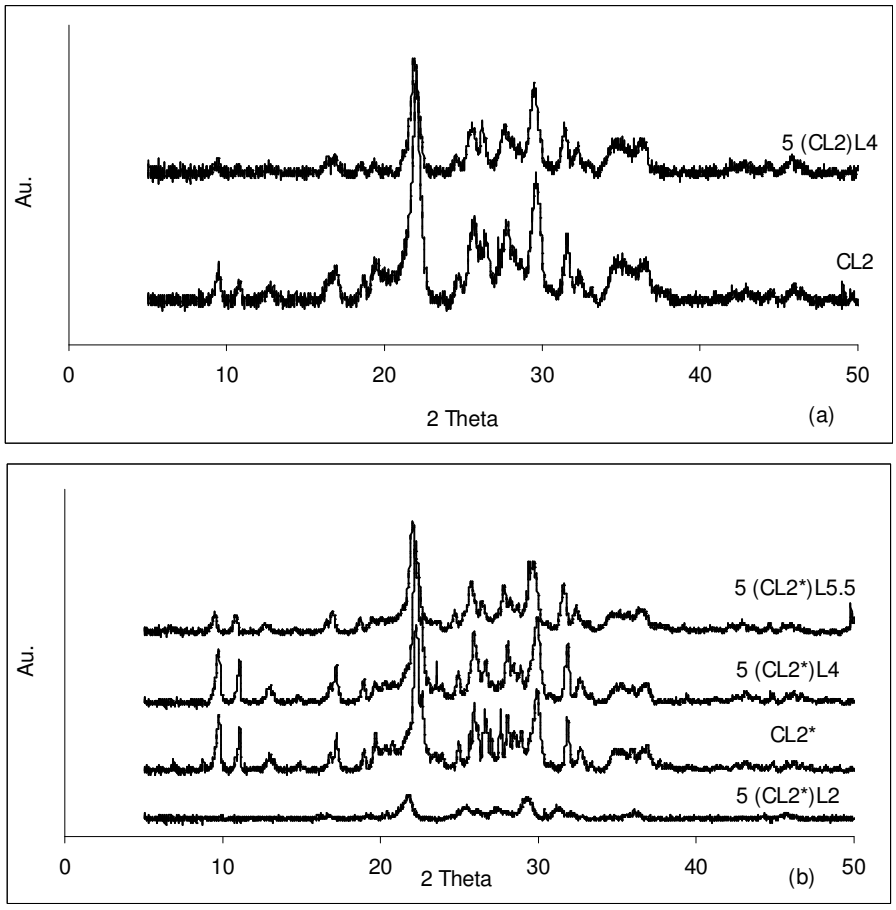

Figure 6.22. X-ray diffraction patterns of the Lactic acid treated zeolites.

The clinoptilolite characteristic peak at 9.8^{o} 2θ disappeared with interaction of zeolite at pH 4 and 2 when starting zeolite is untreated and modified respectively.

Figure 6.23. presents the XRD patterns for the zeolite after treatment at basic electrolyte pH. One significant observation for this pattern is that the peaks assigned to the clinoptilolite species significantly increased for 1 (CL2)S. The peak at 2θ=9.8^{o} was than decreased with increasing zeolite 5%. Whereas neither the Si/Al ratio nor the dissolution of Si and Al were the highest for this zeolite content.

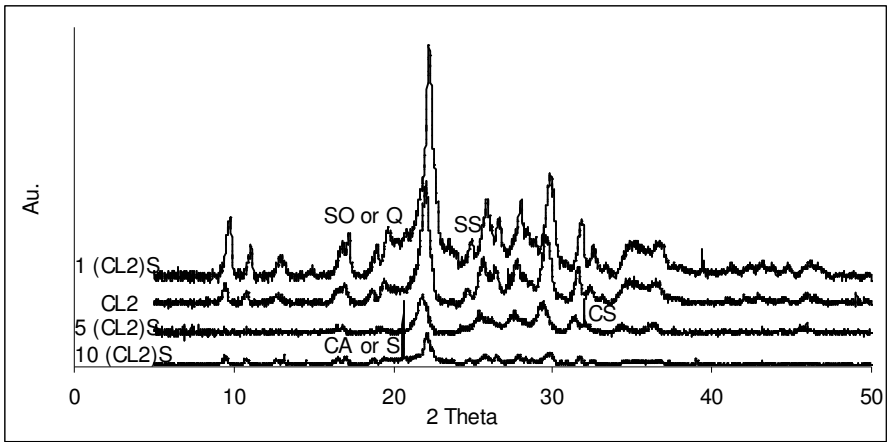

Figure 6.23. X-Ray diffraction pattern of untreated and sodium hydroxide treated zeolites.

Some different peaks were observed depending on complexion and precipitation of metal hydroxide for the samples as displayed by Figure 6.23. The possibilities of these peaks were given as follows.

1(CL2)S : 23.67^{o}; Sodium aluminum silicate Na64Al54Si138O3 (SS), 20.79^{o}; quartz (SiO2) (Q) or sodium aluminum oxide ($NaAlSiO_4$) (SO)

5 (CL2)S: 32.1^{o}; calcium silicate oxide ($Ca3(SiO_4)O$) (CS)

10(CLS)S: 20.06^{o}; Calcium Aluminum oxide or sodium iron silicon oxide ($Na0.68Fe0.68Si0.32O_2$) (CA or SI)

6.3.2 FTIR Studies

FTIR spectrums of the HCl treated zeolites are presented in Figure 6.24. The O–T–O stretching vibration band at 1047 cm^{-1} is sensitive to the content of the framework silicon and aluminum.

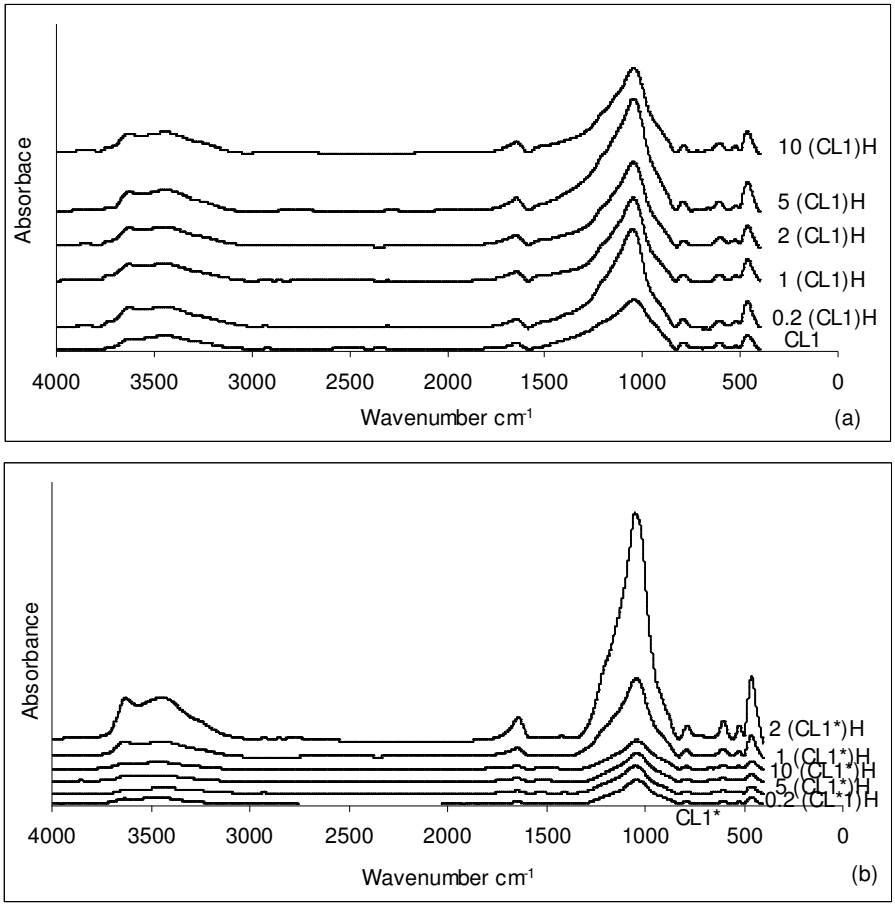

Figure 6.24. FTIR spectra of the hydrochloric acid treated zeolites.

The dissolution of Al and Si from zeolite framework during equilibration periods resulted in an increase in this band frequency. The band at 1047 cm^{-1} for untreated zeolite shifts towards to the higher frequency (1055 cm^{-1} and 1051 cm^{-1}) for zeolite content of 0.2 and 1 % respectively. On the other hand the similar effect on the modified zeolites was not observed. The relative intensities of the IR bands, especially 1047/465 cm^{-1} and 604/465 cm^{-1} can give some information about degree of crystallinity as mentioned in Chapter 4. The ratio of the bending vibration (observed at 605 cm^{-1}) to the band at 465 cm^{-1} $I_{604/465}$ associated with amorphous structure was decreased for all samples, the highest for the smallest amount (0.2 %).

According to UV analysis the activity of pepsin enzyme was decreased due to the absorbing by natural clinoptilolite. To confirm this IR spectrum of zeolites treated with SGJ solution was analyzed. No relevant changes or no new peaks of the as-received zeolites was observed after the treatment as displayed in Figure 6.25.(a). However in the experiment conducted with (0.5 %) modified zeolite the intensity of

Na_2CO_3 peak at 1498 cm^{-1} was decrease. The complex formed on the carbonated sites is responsible for this decrease.

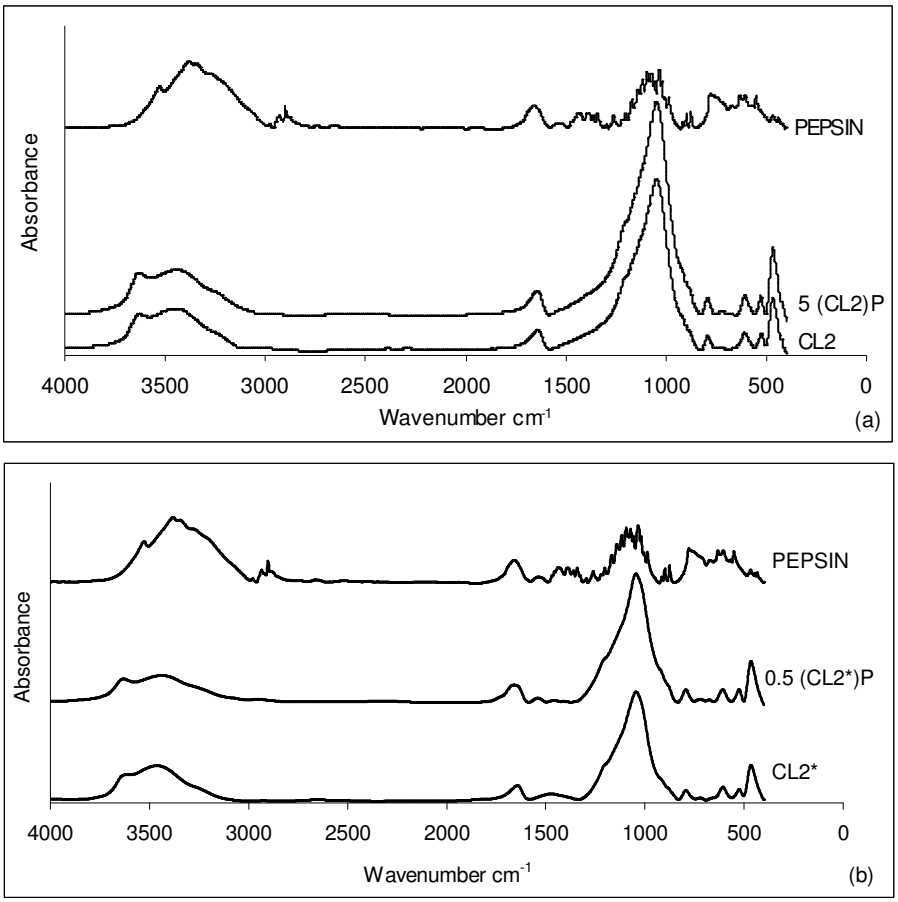

Figure 6.25. FTIR spectra of synthetic gastric juice treated zeolites.

The shift at 1047 cm^{-1} band was not observed for untreated and modified zeolite indicating that the removal of Al and Si was very low level. This result also confirmed by the chemical analysis of solution.

In comparison of the FTIR spectrums of untreated and Acetic acid treated no shift was observed at 1047 cm^{-1} band to higher frequency indicating the framework dealumination did not occurred (Figure 6.26.). The absorption of acetate ions (CH_3COO^-) was not detected from FTIR spectrum.

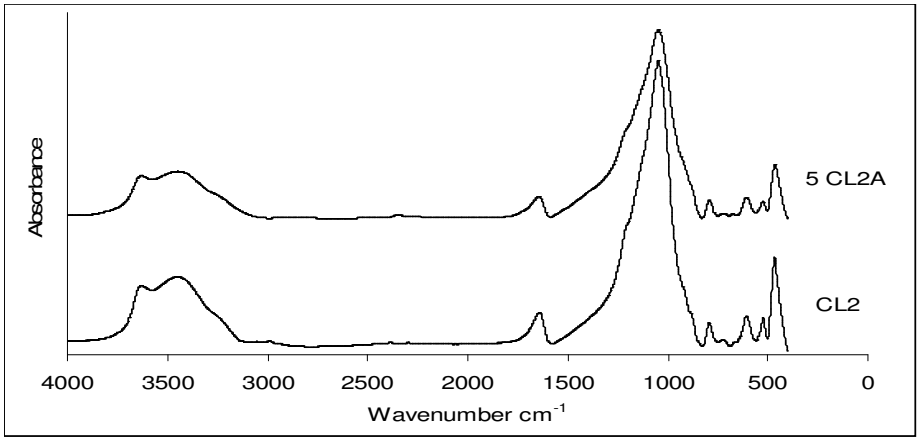

Figure 6.26. FTIR spectrum of the untreated and acetic acid treated zeolite.

Although the band intensities decreased in the lactic acid treated zeolites, the shift in the FTIR spectrums of the zeolite obtained was not observed (Figure 6.27.). The band at 1498 cm^{-1} indicating the vibration of the carbonate, which is characteristics for the pretreated zeolite disappeared when the zeolite treated with the solution pH_i 2 (Figure 6.27.(b)). This shows the carbonate attached on the modified zeolite was dissolved at the lowest pH (pH 2).

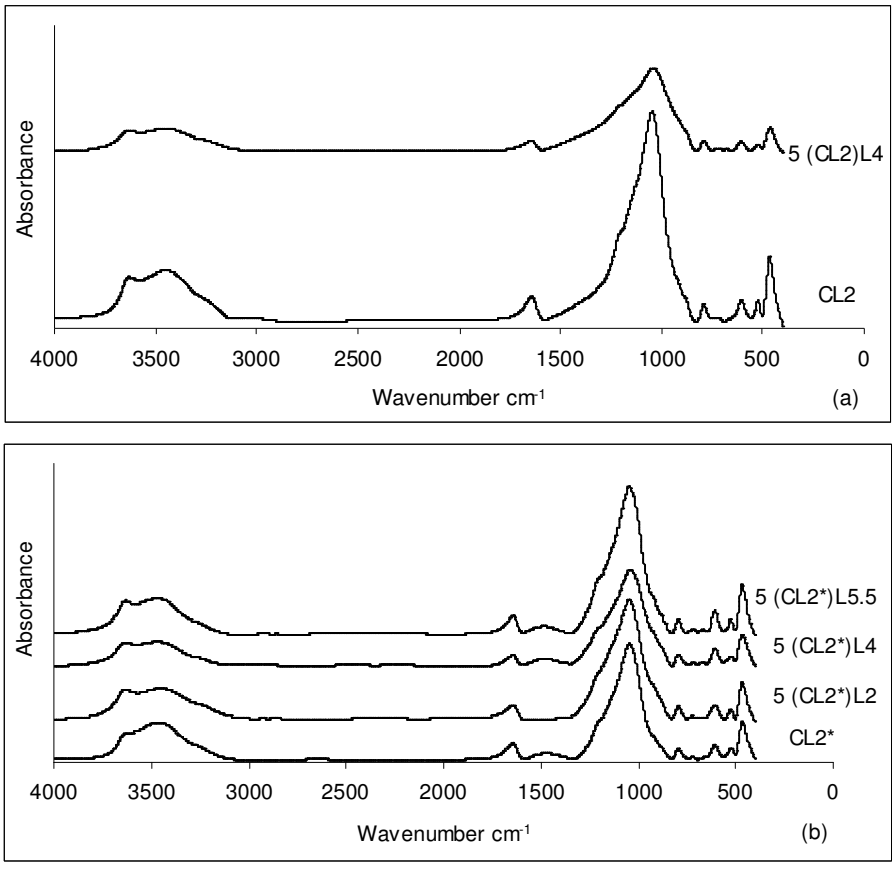

Figure 6.27. FTIR spectra of the Lactic acid treated zeolites.

Figure 6.28. shows the FTIR absorbance spectra of the untreated (as-received) zeolite before and after NaOH treatment.

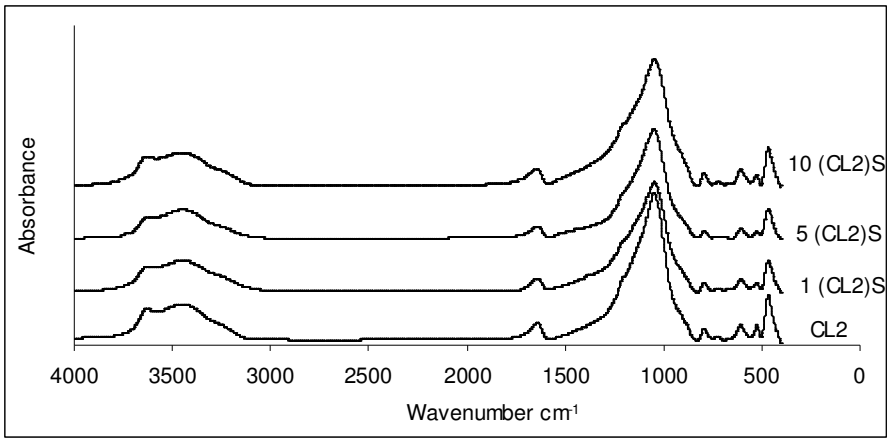

Figure 6.28. FTIR spectra of untreated and sodium hydroxide treated zeolites.

IR spectra do not show significant change in the zeolite structure indicating the high stability of it against to NaOH treatment.

6.3.3. TGA Studies

Figure 6.29. shows the weight loss of the zeolite taken from HCl solution. The peak at 680 ^{o}C attributed the carbonate (for CL1*) almost disappeared due to dissolution of the carbonate in the dilute HCl solution. The available proton to dissolve the carbonate into zeolite is constant. By considering to solve the more amount carbonate the more amount of proton needed.

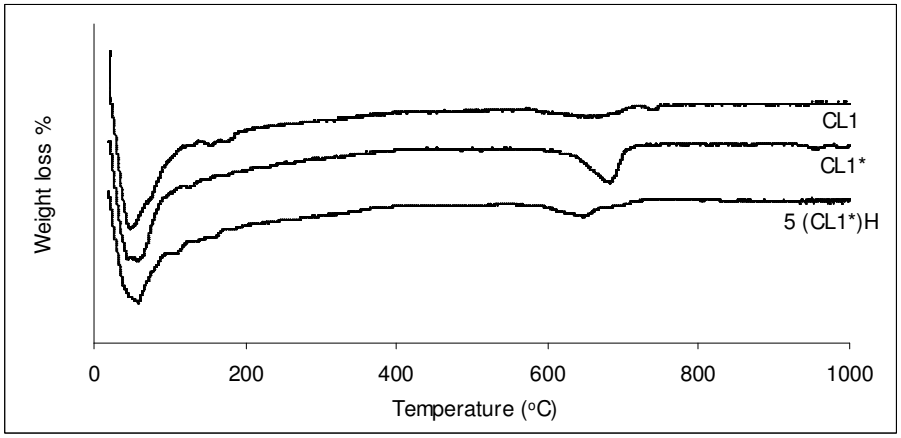

Figure 6.29. DTGA curves of hydrochloric acid treated zeolites.

The lactate ionized (partially) is possible sorbed on the zeolite surface. This can be understood from TGA curves given in Figure 6.30. Two peaks between 100 and 400 ^{o}C are related to lactate bounded on the surface.

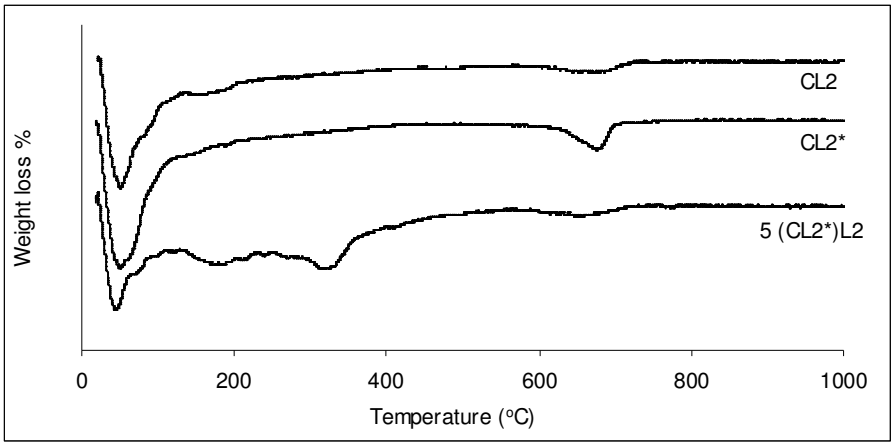

Figure 6.30. DTGA curves of lactic acid treated zeolites.

6.3.4. ZP Studies

Zeta potential measurement was performed and presented in Table 6.18. for the starting and acid or alkali treated zeolite. The samples treated in acid or base solution with the concentration of 5 % were investigated if there was a change in their surface charge or not. The surface charge of the as-received zeolite is almost the same with the surface charge of zeolite (-25 mV at about pH=6.2) used in the study performed by Ersoy and Çelik (2002). It was obtained that there is no significant differences between the surface potential of as-received, modified and acid or alkali treated zeolites. This is indicating that zeolites tend to equilibrate their surface charge without ignoring the properties of electrolyte solution. However if changes had been significant, then zeolite would have been difficult in making their surface charge constant.

Table 6.18. The surface charge of starting and acid or alkali treated zeolites.

Zeolites	**Surface charge (mV)**	**Standard deviation**
As-received	-24.90	± 0.96
Modified	- 24.63	± 0.64
5 (CL1)H	-25.43	± 1.26
5 (CL1*)H	-24.40	± 0.64
5 (CL2)A	-25.67	± 1.20
5 (CL2)S	-23.77	± 1.42
5 (CL2*)L2	-23.40	± 1.40

CHAPTER 7

CONCLUSIONS

The study in which the chemical behavior of the natural and Na_2C0_3 treated zeolitic material was investigated by varying zeolite amount in aqueous medium of HCl, SGJ, NaOH, CH_3COOH, and $CH_3CHOHCOOH$. The following results was reached

- Untreated zeolite used in the study increased the pH from 2 to 3.6 in HCl solution and decreased the pH from 11.2 to 8.5 in NaOH solution for 10 % zeolite content (w/v) because of the amphoteric behavior of zeolitic material. However neutralizing capacity of used zeolites was lower when compared to the zeolite used in the study performed by Ersoy and Çelik (2002) depending on the clinoptilolite content (90-92 %).
- The zeolite content of the solution is effective on pH evolution.
- The effect of untreated zeolite amount on equilibrium pH of HCl solution was linearly increase with increasing solution pH while for modified ones at above the concentrating of 2 % it is the same. This is because the total amount of proton and hydroxide remain in the solutions are the same and no removal of carbonate anions at pH=8.
- The proton or hydroxide ions entered to the zeolite could not balance the cations released from zeolite structure. Therefore not only ion exchange, but also the other mechanism took place.
- In acidic medium besides to ion exchange, sorption (of proton to form inner and/or outer complex), and dissolution occurred.
- At low zeolite concentration ion exchange and adsorption, at high concentration cation hydrolysis and complexion mechanism were dominant.
- An application of the modified zeolite as solid buffer in SGJ solution shows that 0.5% (w/v) of zeolite concentration can be used for treatment of gastric disturbance. A significant loss in pepsin activity (<18%) was not detected for this zeolite concentration.

- In the pH evolution of acid solution, the modified zeolite pretreated by using the Na_2CO_3 was more effective than as-received form of the zeolite (untreated) due to the increase of OH^- ion concentration with the formation of bicarbonate.
- A significant increase in total exchange capacity (from 2.49 and 2.77 to 3.06 and 3.78 meq/g for CL1, CL2, CL1* and CL2* respectively) was obtained when the zeolite was modified with Na_2CO_3 solution. However the washing step applied after modification has negative effect on TEC of zeolite.
- The decrease of solution pH in NaOH solution was due to the adsorption of hydroxyl ions (deprotonation) or inner-outer surface complexion of Na^+ ion with zeolite surface. As a result of complexion reaction, H^+ ion is generated resulting in more decrease in solution pH (as in 1 (CL2)S)
- In basic medium, the cation release was at the highest level when compared to hydroxyl transferred to zeolite without loss in the crystalline structure of zeolite. This results from the less dissolution of the framework aluminum. The hydroxide leads to hydrolysis of cation to form outer surface complex.
- Diffusion of hydroxide was rapid when compared to diffusion of hydrogen to the zeolite surface ($10.8x10^{-16}$ and $42.61x10^{-17}$ for 5(CL2)S and 5(CL1)H respectively).
- For all treatments the amount of exchange or release cations was mostly Na^+ ion due to its weaker bond and located channels in zeolite structure.
- Dissolution of Al and Si was not observed except in strong electrolyte acid solution (HCl) at low zeolite concentration. The reason for that is the strong interaction of proton to the surface hydroxyl groups.
- Some new peaks were observed in XRD studies for NaOH and HCl treated zeolites (at high zeolite concentration) because of surface complexion.
- In FTIR studies there was no shift at 1047 cm^{-1} band observed except the low concentration of zeolites treated with HCl confirming dissolution of Al and Si.
- According the FTIR analysis, the band at 1498 cm^{-1} related to carbonate did not changed when modified zeolites was treated with $C_3H_6O_3$ at pH_i=4 and 5.5 but decrease when pH_i=2. Because carbonate anions could not removed from the surface at neutral or basic solution pH.
- In the treatment of $C_3H_6O_3$, lactate anions formed with the ionization of lactic acid. The proton was consumed for exchange or adsorption while lactate anion

precipitate to surface (as calcium or sodium lactate) by complexion mechanism as confirmed by TGA analysis.

- The results obtained from XRD and FTIR analysis lead us to consider that the untreated and modified NZ from two different deposit (Gordes) is stable as a solid buffer in acidic (strong and weak) and basic solution. Under basic condition, in NaOH solution the zeolite did not convert to zeolites such as analsime, feldspar, and NaP zeolite as stated in the literature. Because NaOH concentration used in this study was very low.
- About 17% and 56% increase and 13 % decrease in specific surface area was obtained by treating the zeolite (5%w/v) with CH_3COOH, HCl and NaOH respectively.
- The surface potential of acid or alkali treated zeolites was not significantly changed.

REFERENCES

Ackley, M.W.; Rege, S.U.; Saxena, H. 2003. "Application of Natural Zeolites in The Purification and Separation of Gases", *Microporous and Mesoporous Materials*. Vol.61, pp. 25-42.

Ackley, M. and Yang, R.T. 1991. "Diffusion in Ion-Exchanged Clinoptilolites", *AIChE Journal*. Vol. 37, pp. 1645-1656.

Akdeniz, Y.; Cation Exchange in Zeolites, Structure Modification by Using Microwave, *M.S. Thesis*, İzmir Institute of Technology, 1999.

Anna, O.; Mohamed, H.; Andreas, K. 2001. "Realumination of Dealuminated HZSM-5 Zeolites by Acid Treatment: A Reexamination", *Microporous and Mesoporous Materials*. Vol. 46, pp. 177-184.

Arcoya, A.; Gonzalez, J.A.; Llabre, G.; Seoane, X.L.; Travieso, N. 1996. "Role of Countercations on The Molecular Sieve Properties of A Clinoptilolite", *Microporous Materials*. Vol. 7, pp. 1-13.

Barrer, R.M.; Barri, S.A.I.; Klinowski, J., 1980. *Journal Chemical Soceity*. Faraday Trans. Vol. 76, p. 1038.

Bekkum, H.V.; Flanigen, E.M.; Jansen J.C., 1991. "Introduction to Zeolite Science and Practice", Vol. 58.

Bish, D.L.; Chipera, S.J. 1995. "Multi-Reflection RIR and Intensity Normalizations for Quantitative Analysis: Application to Feldspar and Zeolites", *Powder Diffraction*. Vol. 10, pp. 47-55.

Breck, D.W., 1974. "Zeolite Molecular Sieve Structure", Chemistry and Use, *Wiley Interscience*. New York.

Castellar, R.M.; Aires-Barros, M.R.; Cabral, M.S.J.; Iborra, J.L. 1998. "Effect of Zeolite Addition on Ethanol Production from Glucose by *Saccharomyces Bayanus", J. Chem. Thechnol. Biotechnol*. Vol. 73, pp. 377-384.

Charistos, D.; Godelitsas, A.; Tsipis, C.; Sofoniou, M. 1997. "Interaction of Natrolite and Thomsonite Intergrowths with Aqueous Solutions of Different Initial pH Values at 25°C in The Presence of KCI: Reaction Mechanisms", *Applied Geochemistry.* Vol. 12, pp. 693-703.

Concebcion-Rosabal, B. and Rodriguez- Fuentes, G. 1997. "Development and Featuring of The Zeolitic Active Principle FZ: A Glucose Adsorbent", *Elsevier Science Inc*. Vol. 19, pp. 47-50.

Doula, M.K. and Ioannou, A. 2002. “Copper Adsorption and Si, Al, Ca, Mg, and Na Release From Clinoptilolite”, *Microporous and Mesoporous Materials*. Vol. 245, pp. 237–250.

Doula, M.K. and Ioannou, A. 2003. “The Effect of Electrolyte Anion on Cu Adsorption–Desorption by Clinoptilolite”, *Microporous and Mesoporous Materials*. Vol. 58, pp. 115–130.

Dyer, A. and White, K.J. 1999. “Cation Diffusion in The Natural Zeolite Clinoptilolite”, *Thermochimica Acta.* Vol. 340-341, pp. 341-348

Ersoy, B. and Çelik, M.S. 2002. “Electrokinetic Properties of Clinoptilolite with Mono- and Multivalent Electrolytes”, *Microporous and Mesoporous Materials*. Vol. 55, pp. 305-312.

Ewing, G.W., 1985. “Instrumental Method of Chemical Analysis”, Fifth edition, London.

Farias, T.; Ruiz-Salvador, A.R.; Rivera, A. 2003. “Interaction Studies Between Drugs and A Purified Natural Clinoptilolite”, *Journal of Colloidal and Interface Science*. Vol. 260, pp. 166-175.

Fifield, F.W. and Kealey D., 2000. “Principle and Practice of Analytical Chemistry”, Fifth edition, London.

Gilreath, E.S., 1954. “Quantitative Analysis Using Semimicro Methods”, New York.

Gomonaj, V.; Gomonaj, P.; Golub, N.; Szekeresh, K.; Charmas, B.; Leboda, R. 2000. “Compatible Adsorption of Strontium and Zinc Ions as well as Witamins on Zeolites”, *Adsorption Science & Technology*. Vol. 18, No. 4, pp. 295-306.

Jentys, A. and Lercher, J.A. 2001. “Techniques of Zeolite Characterization”, *Introduction to Zeolite Science and Practice Elsevier*. Amsterdam, pp. 345-386.

Kovatcheva-Ninova, V. and Dimitrova, D. 2002. “Studies the Impact of Low-Frequency Acoustic Field Upon Cation Exchange Capacity of Natural Zeolite”, *Mining and Mineral Processing*. Vol. 44-45, part II, pp. 99-103.

Kurama, H.; Zimmer, A.; Reschetilowski, W. 2002. “Chemical Modification Effect on The Sorption Capacities of Natural Clinoptilolite”, *Chemical Engineering Technology*. Vol. 25, pp. 301-305.

Lawes, G., 1987. “Scanning Electron Microscopy and X-Ray Microanalysis”, New York.

Liberatore, P.A. 1993. “Determination of Majors in Geological Samples by ICP-AES”, ICP-12.

Mirela, R.; Stefanovic, S.C.; Curkovic, L. 2002."Evaluation of Croatian Clinoptilolite- and Montmorillonite-Rich Tuffs for Ammonium Removal", *Croatica Chemica Acta*. Vol 75, No.1, pp. 255-269.

Mozgava, W.; Sitarz, M.; Rokita, M 1999. "Specroscopic Studies of Different Aluminosilicate Structure", *Journal of Molecular Structure*. Vol. 511-512, pp. 251-257.

Mozgava, W. 2001. "The Relation Between Structure and Vibrational Spectra of Natural Zeolites", *Journal of Molecular Structure*. Vol. 596, pp. 129-137.

Mumpton, F.A. 1999. "Uses of Natural Zeolites in Agriculture and Industry", *Proc. Natl. Acad. Sci*. Vol. 96, pp. 3463–3470.

Oumi, Y.; Nemoto S.; Nawata, S.; Fukushima, T.; Teranishi, T.; Sano, T. 2002. "Effect of The Framework Structure on The Dealumination–Realumination Behavior of Zeolite", *Materials Chemistry and Physics*. Vol. 78, pp. 551–557.

Özkan, F.C. and Ülkü, S. 2004. "The Effect of HCl Treatment on Water Vapor Adsorption Characteristics of Clinoptilolite Rich Natural Zeolite", *Microporous and Mesoporous Materials*. Vol, 77, pp. 47–53.

Petrus, R. and Warchoł, j. 2003. "Ion Exchange Equilibria Between Clinoptilolite and Aqueous Solutions of Na^+/Cu^{2+}, Na^+/Cd^{2+} and Na^+/Pb^{2+}", *Microporous and Mesoporous Materials*. Vol. 61, pp. 137–146.

Ponizovsky, A.A. and Tsadilas, C.D. 2003. "Lead(II) Retention by Alfisol and Clinoptilolite: Cation Balance and pH Effect", *Geoderma.* Vol. 115, pp. 303–312.

Praustnitz, J.M.; Lichtenthaler, R.N.; Azevedo, E.G., 1999. "Molecular Thermodynamics of Fluid-Phase Equilibria", London

Rivera A.; Rodriguez- Fuentes G.; Altshuler E. 2000. "Time Evolution of A Natural Clinoptilolite in Aqueous Medium: Conductivity and pH Experiments", *Microporous and Mesoporous Materials*. Vol. 40, pp. 173-179.

Rivera A.; Rodriguez-Fuentes G.; Altshuler E. 1998. "Characterization and Neutralizing Properties of A Natural Zeolite/Na_2CO_3 Composite Material", *Microporous and Mesoporous Materials.* Vol. 24, pp. 51-58.

Rivera-Garza, M.; Olguin, M.T.; Garcia-Sosa, I.; Alcantara, D.; Rodriguez-Fuentes, G. 2000. "Silver Supported on Natural Mexican Zeolite as an Antibacterial Material", *Microporous and Mesoporous Materials.* Vol 39, pp. 431-444.

Sandler, S.I., 1999. "Chemical and Engineering Thermodynamics", Third edition, New York.

Tarasevich, Y.I.; Krysenko, D.A.; Polyakov, V.E. 2002. "Selectivity of Low- and High-Silica Clinoptilolites With Respect to Alkali and Alkaline–Earth Metal Cations", *Colloid Journal.* Vol. 64, No. 6, pp. 759–764.

Top. A.; Cation Exchange (Ag^{+}, Zn^{2+}, Cu^{2+}) Behavior of Natural Zeolites, *M.S. Thesis*, İzmir Institute of Technology, 2001.

Top, A. and Ülkü, S. 2004. "Silver, Zinc, and Copper Exchange in A Na-Clinoptilolite and Resulting Effect on Antibacterial Activity", *Applied Clay Science.*

Trgo, M. and Peric, J. 2003. "Interaction of The Zeolitic Tuff with Zn-Containing Simulated Pollutant Solutions", *Microporous and Mesoporous Materials*. Vol. 61, pp. 117-125.

Tsitsishvili, G.V.; Andronikashvili, T.G.; Kirov, T.G.; Filizova, L.D., 1992. "Natural Zeolites", Ellis Horwood, New York.

Türkmen, M.; Removal of Heavy Metals From Waste Waters by Use of Natural Zeolites, *M.S. Thesis*, İzmir Institute of Technology, 2001.

Ülkü, S. 1984. "Application of Natural Zeolite in Water Treatment", Umvelt'84.

Valverde, J.L.; Lucas, A.; Gonzalez, M.; Rodrıguez, J.F. 2001. "Ion-Exchange Equilibria of Cu^{2+}, Cd^{2+}, Zn^{2+}, and Na^{+} Ions on The Cationic Exchanger Amberlite IR-120", *J. Chem. Eng. Data*. Vol. 46, pp. 1404-1409.

Weitkamp, J. and Puppe, L. 1999. "Catalysis and Zeolites: Fundamental and Applications", New York.

APPENDIX A

REFERENCE INTENSITY RATIO (RIR) METHOD

The natural zeolitic material used in this study (CL1 and CL2) was characterized by X-Ray diffraction techniques using CuKα radiation in the range of 2θ: 2^o-40^o with 0.2^o step size. The zeolitic material having 30.30 and 23.62 μm particle size was decreased at least to 10 μm by grinding with an agate. This is necessary for the accuracy of the analysis (Bish and Chipera 1995).

Quantitative determination of crystal phases using XRD is widely used and one of the most common ones Relative Intensity Ratio (RIR) methods because of obtaining reliable results. This method has been measured for one or more reflection for each phase to be analyzed before analysis of unknowns. RIR method can be defined as the intensity of a peak of interest for a given phase divided by the intensity of a peak from a standard in a 50:50 mixture (Bish and Chipera 1995).

In order to determine the clinoptilolite content of zeolitic materials used in this study two separate intensity region were chosen : the 020 reflection at 9.8^o 2θ and the sum of the intensity in the range 22.1-23^o 2θ. As standard zeolites taken from Idaho (IDA) and California (CAL) was used. A-alumina powder (corundum) was also used as the internal standard. The highest peak for corundum is at 35.21^o 2θ. Two RIR standard (IDA and CAL) were prepared by mixing with corundum (50:50). XRD spectrum of six replicates was run.

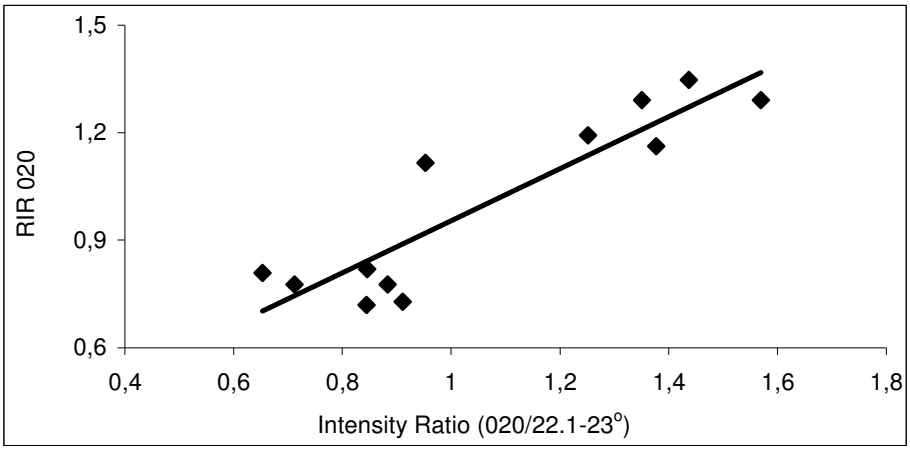

Figure A.1. RIR normalization curve for quantitative determination.

Figure A.1. was plotted by measuring RIR value for the 020 reflection versus the intensity ratio between 020 reflection and the (22.1-23^{o} 2θ) sum peak for each of two clinoptilolite standard. From improved RIR curve, analysis of unknown clinoptilolite content of zeolitic materials can be obtained. The equation expressed below was obtained by the help of intensity ratio and corresponding RIR values.

$$RIR_{020} = 0.7261*(INT_{020}/INT_{22.1\text{-}23^{o}}) + 0.2287$$

The natural zeolitic material used in this study was determined as 55.5 and 58.5 % for CL1 and CL2 respectively as a result of the RIR techniques.

APPENDIX B

PARTICLE SIZE MEASUREMENTS WITH SEDIGRAPH

Sedimentation is a technique for determining the particle size. This technique can be applied by sedigraph which is X-ray based method. In this study Micromeritics Sedigraph 5100 was used in order to determine the particle size of starting zeolites (CL1 and CL2). The zeolites were mixed with a viscosity specific fluid (0.05 % calgon solution) which allows the particles to go into the solution. Zeolite containing solutions put into ultrasonic bed for 15 minutes in order to disaggregate the small particles which agglomerate on the big particles. In this method X-ray intensity was used to determine the settling rate and calculate the particle size distribution. The particle size distribution of starting zeolites is shown in Figure A.2.

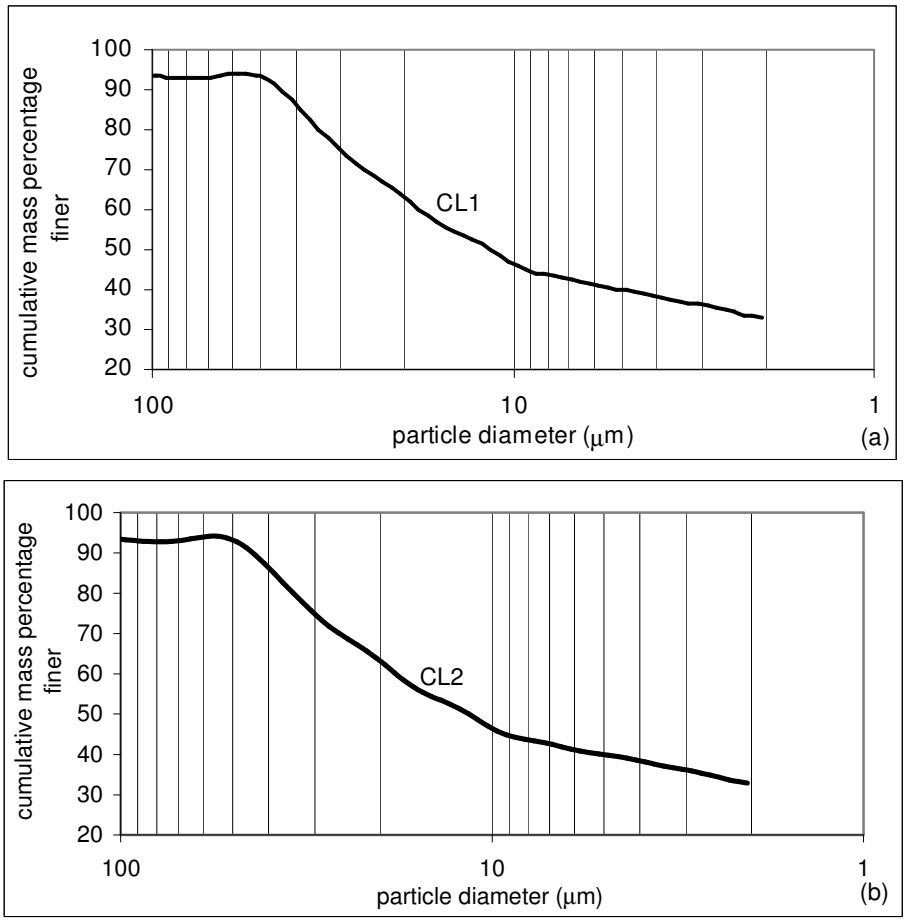

Figure B.1. Particle size distribution of starting zeolites (a) CL1 and (b) CL2.

According to the sedimentation analysis particle size of starting zeolite was 30.30 and 23.62 μm for CL1 and CL2 respectively. The values are not in the range of 38-106 μm because of dry sieving. Dry sieving can not prevent agglomeration of small particle on bigger ones.